FAST MULTIPOLE METHOD FOR 3-D HELMHOLTZ EQUATION IN LAYERED MEDIA[*]

BO WANG[†], WENZHONG ZHANG[‡], AND WEI CAI[§]

Abstract. In this paper, a fast multipole method (FMM) is proposed to compute long-range interactions of wave sources embedded in 3-D layered media. The layered media Green's function for the Helmholtz equation, which satisfies the transmission conditions at material interfaces, is decomposed into a free space component and four types of reaction field components arising from wave reflections and transmissions through the layered media. The proposed algorithm is a combination of the classic FMM for the free space component and FMMs specifically designed for the four types reaction components, made possible by new multipole expansions (MEs) and local expansions (LEs) as well as the multipole-to-local translation (M2L) operators for the reaction field components. Moreover, equivalent polarization source can be defined for each reaction component based on the convergence analysis of its ME. The FMMs for the reaction components, implemented with the target particles and equivalent polarization sources, are found to be much more efficient than the classic FMM for the free space component due to the fact that the equivalent polarization sources and the target particles are always separated by a material interface. As a result, the FMM algorithm developed for layered media has a similar computational cost as that for the free space. Numerical results validate the fast convergence of the MEs and the $O(N)$ complexity of the FMM for interactions of low-frequency wave sources in 3-D layered media.

Key words. fast multipole method, layered media, multipole expansions, local expansions, Helmholtz equation, equivalent polarization sources

AMS subject classifications. 15A15, 15A09, 15A23

1. Introduction. The fast multipole method (FMM) has been a revolutionary development in modern computational algorithms for treating many-body interactions. In fact, it was considered one of the top 10 algorithms in the 20th century [10]. The FMM can reduce the $O(N^2)$ cost of computing long-range interactions (Columbic electrostatics, wave scattering) among N particles (or sources) to $O(N)$ or $O(N \log N)$. Such a capability of the FMM has had a tremendous impact on modern computational biology, astronomy, and computational acoustics and electromagnetics, among many other applications in sciences and engineering. The original FMMs developed by Greengard and Rokhlin [16, 17] for particles in the free space are based on multipole expansions (MEs) for a Green's function $G(\boldsymbol{r}, \boldsymbol{r}')=G(\boldsymbol{r} - \boldsymbol{r}')$ to achieve a low-rank representation for the long-range interactions between sources. The MEs for the wave interactions were made possible by the Graf's addition theorem for Bessel functions. As a simple way to view the ME, we split the argument of the Green's function, the zeroth order Bessel function for wave interactions, as $G(\boldsymbol{r} - \boldsymbol{r}') = G((\boldsymbol{r} - \boldsymbol{r}_c) + (\boldsymbol{r}_c - \boldsymbol{r}'))$ where $\boldsymbol{r}_c$ is selected as the center of many sources $\boldsymbol{r}'$ while $\boldsymbol{r}$ is any field location far away (well-separated) from all sources. The Graf's addition theorem gives an expansion of G in terms of separable terms involving $(\boldsymbol{r}-\boldsymbol{r}_c)$

and $(r_c - r')$, respectively. Terms involving $(r - r_c)$ will appear as the higher order multipoles, i.e., higher order Bessel functions, while terms with $(r_c - r')$ for each source r' contributes to the ME expansion coefficients. For a far field location r, such an expansion exhibits exponential convergence, thus only a small number of p terms, therefore p ME-coefficients, are needed, resulting in a p-term low-rank approximation for the far field of many sources.

As the original FMM was developed based on far field approximations by MEs obtained by the Graf's addition theorem applied to free space Green's functions, we can understand the difficulties of extending this approach to sources embedded in layered media, which are ubiquitous in computer engineering, geophysical, and medical image applications. For those applications, Green's functions for layered media (layered Green's functions) are preferred to describe the interactions to avoid introducing artificial unknowns on the infinite material interfaces. Unfortunately, in those cases, no theory like Graf's addition theorem is available for layered Green's functions. For this reason, the ME-based FMM of Greengard and Rokhlin has not been extended to layered Green's functions due to the lack of corresponding multipole expansions of the far field of wave sources in general multi-layered media. In our recent work [9], MEs for the case of an impedance 2-D half space were obtained by using an analytical image representation of the layered Green's function, which however are not available for general multi-layered media. Then, in our more recent work [38], MEs and multipole to local (M2L) translation operators were developed for 2-D Helmholtz equations in general layered media. In a different approach, an inhomogeneous plane wave fast method was developed [19] by approximating the Green's function with plane waves sampled along a steepest descent path in the complex wave number space. So far, to handle the wave interaction of sources embedded in general layered media using layered Green's functions, some other fast methods have been proposed such as FMM using Taylor expansion-based low-rank representation of Green's function [32][31], and cylindrical wave decomposition of the Green's function together with 2-D FMMs for cylindrical waves [8]. On the other hand, kernel independent compression techniques [37] [33] could also be considered for the layered Green's functions.

In this paper, we will develop MEs and local expansions (LEs) for general layered Green's function for 3-D Helmholtz equations as well as relevant M2L operators (thus extending our previous results for 2-D Helmholtz equations [38]), providing the key ingredients in the hierarchical design of the 3-D FMM. The layered Green's function is decomposed into a free space part and four reaction fields arising from wave reflections and transmissions through the layered media. Our approach relies on two technical identities, the first one expresses the layered Green's functions in terms of Sommerfeld integral involving plane waves, and the second one is the Funk-Hecke identity, which expresses plane waves in terms of cylindrical waves (Bessel functions). With the separable property of plane waves as well as the Funk-Hecke identity, we are able to derive the MEs and LEs for the layered Green's functions in 3-D as well as the M2L operators. As shown in [38], the convergence of the far field for the reaction field component of the layered Green's function in fact depends on the distance between the target and the location of some kind of polarization source, which can be defined for each reaction component (see (61) and Fig. 5). Therefore, in the implementation of the FMM for the reaction field components, the original and the polarization sources will be combined and embedded into a rectangular box, upon which the oct-tree structure will be built and the FMM can be implemented. As a result, the FMM for the free space can be extended straightforwardly to layered Green's functions. Numerical results will show the fast convergence of the MEs and LEs for the layered

Green's function as well as the $O(N)$ efficiency for 3-D low-frequency acoustic wave interactions.

The rest of the paper is organized as follows. In section 2, we will re-derive the ME, LE and relevant M2L operators for the free space Green's function using the new approach discussed above. The same technique will be then applied to layered Green's functions. Section 3 gives the derivation of ME, LE and M2L operators for layered Green's functions, given as Sommerfeld integrations of plane waves. A FMM based on the new ME, LE and M2L operator for reaction components is then presented. Section 4 gives numerical results for sources in three layers media. Various efficiency comparisons are given to show the performance of the proposed FMM. Finally, conclusion and discussions are given in Section 5.

2. A new derivation for h- and j-expansions of the free space Green's function of 3-D Helmholtz equation and translations. In this section, we first review the h- and j-expansions, namely the multipole and local expansions, for the free space Green's function of the Helmholtz equation and the translation from a h-expansion to a j-expansion. They are the key formulas in the free space FMM and can be derived by using the well-known addition theorems for regular and singular wave functions. Then, we will introduce a new derivation for the h- and j-expansions by using an integral representation of Hankel functions. This new technique will be applied to derive multipole and local expansions for reaction components of layered Green's functions in the next section.

2.1. The h- and j-expansions of free space Green's function. Let us first recall the addition theorems for regular and singular wave functions. Suppose $\boldsymbol{r}_j = (r_j, \theta_j, \varphi_j)$ is the position vector of a point P in spherical coordinates with respect to a given center O_j for $j = 1, 2$, and $\boldsymbol{b} = (b, \alpha, \beta)$ is the position vector of O_1 with respect to O_2, such that $\boldsymbol{r}_2 = \boldsymbol{r}_1 + \boldsymbol{b}$. Meanwhile, the spherical harmonics are defined as

$$(1) \qquad Y_n^m(\theta, \varphi) = (-1)^m \sqrt{\frac{2n+1}{4\pi} \frac{(n-m)!}{(n+m)!}} P_n^m(\cos\theta) e^{\mathrm{i}m\varphi} = \widehat{P}_n^m(\cos\theta) e^{\mathrm{i}m\varphi},$$

where $0 \le |m| \le n$ and $P_n^m(\cos\theta)$ is the associated Legendre function and $\widehat{P}_n^m(\cos\theta)$ is its normalized version. We will use the following addition theorems [24].

THEOREM 1. *Let $z_\nu(\omega)$ be any spherical Bessel function of order ν, that is*

$$z_\nu(\omega) = j_\nu(\omega), y_\nu(\omega), h_\nu^{(1)}(\omega), \text{ or } h_\nu^{(2)}(\omega).$$

Let $\boldsymbol{r}_2 = \boldsymbol{r}_1 + \boldsymbol{b}$. Then

$$(2) \ \ z_0(kr_2) = \begin{cases} 4\pi \displaystyle\sum_{n=0}^{\infty} \sum_{m=-n}^{n} (-1)^n z_n(kb)\overline{Y_n^m(\alpha, \beta)} j_n(kr_1) Y_n^m(\theta_1, \varphi_1), & \text{if } r_1 < b, \\ 4\pi \displaystyle\sum_{n=0}^{\infty} \sum_{m=-n}^{n} (-1)^n j_n(kb)\overline{Y_n^m(\alpha, \beta)} z_n(kr_1) Y_n^m(\theta_1, \varphi_1), & \text{if } r_1 > b. \end{cases}$$

The special case of the above theorem when $z_0 = j_0$ was proved by Clebsch in 1863, see [34, p.363]. According to Watson, another special case with $z_0 = y_0$ was due to Gegenbauer.

THEOREM 2. *Let $\boldsymbol{r}_2 = \boldsymbol{r}_1 + \boldsymbol{b}$. Then*

$$(3) \qquad j_n(kr_2) Y_n^m(\theta_2, \varphi_2) = \sum_{\nu=0}^{\infty} \sum_{\mu=-\nu}^{\nu} \widehat{S}_{n\nu}^{m\mu}(\boldsymbol{b}) j_\nu(kr_1) Y_\nu^\mu(\theta_1, \varphi_1),$$

where

$$(4) \qquad \widehat{S}_{n\nu}^{m\mu}(\boldsymbol{b}) = 4\pi(-1)^m \mathrm{i}^{\nu-n} \sum_{q=0}^{\infty} \mathrm{i}^q j_q(kb) \overline{Y_q^{\mu-m}(\alpha,\beta)} \mathcal{G}(n,m;\nu,-\mu;q),$$

with $\mathcal{G}(n,m;\nu,-\mu;q)$ being the Gaunt coefficient.

THEOREM 3. *Let $\boldsymbol{r}_2 = \boldsymbol{r}_1 + \boldsymbol{b}$. Then*

$$(5) \qquad h_n^{(1)}(kr_2)Y_n^m(\theta_2,\varphi_2) = \sum_{\nu=0}^{\infty} \sum_{\mu=-\nu}^{\nu} S_{n\nu}^{m\mu}(\boldsymbol{b}) j_\nu(kr_1) Y_\nu^\mu(\theta_1,\varphi_1),$$

for $r_1 < b$, and

$$(6) \qquad h_n^{(1)}(kr_2)Y_n^m(\theta_2,\varphi_2) = \sum_{\nu=0}^{\infty} \sum_{\mu=-\nu}^{\nu} \widehat{S}_{n\nu}^{m\mu}(\boldsymbol{b}) h_\nu^{(1)}(kr_1) Y_\nu^\mu(\theta_1,\varphi_1),$$

for $r_1 > b$, where $\widehat{S}_{n\nu}^{m\mu}(\boldsymbol{b})$ is given by (4) and

$$(7) \qquad S_{n\nu}^{m\mu}(\boldsymbol{b}) = 4\pi(-1)^m \mathrm{i}^{\nu-n} \sum_{q=0}^{\infty} \mathrm{i}^q h_q^{(1)}(kb) \overline{Y_q^{\mu-m}(\alpha,\beta)} \mathcal{G}(n,m;\nu,-\mu;q),$$

and $\mathcal{G}(n,m;\nu,-\mu;q)$ is a Gaunt coefficient.

The Gaunt coefficient $\mathcal{G}(n,m;\nu,-\mu;q)$ is defined using the Wigner $3-j$ symbol as follows

$$(8) \qquad \mathcal{G}(n,m;\nu,\mu;q) = (-1)^{m+\mu}\mathcal{S} \begin{pmatrix} n & \nu & q \\ 0 & 0 & 0 \end{pmatrix} \begin{pmatrix} n & \nu & q \\ m & \mu & -m-\mu \end{pmatrix},$$

where $\mathcal{S} = \sqrt{(2n+1)(2\nu+1)(2q+1)/(4\pi)}$. Although we have explicit formulas (4) and (7) for the separation matrices $\widehat{S}_{n\nu}^{m\mu}(\boldsymbol{b})$ and $S_{n\nu}^{m\mu}(\boldsymbol{b})$, they are too complicated to be used directly for practical computations. Fortunately, recurrence formulas are available for their computations (cf. [6, 18]).

With these addition theorems, we can present the h- and j-expansions, which are also named as multipole and local expansions in the FMM. Consider the free space Green's function of the Helmholtz equation with a source and a target at $\boldsymbol{r}' = (x',y',z')$ and $\boldsymbol{r} = (x,y,z)$, respectively. By using the addition Theorem 1, we have an h-expansion (multipole expansion) with respect to a (source) center $\boldsymbol{r}_c^s$:

$$(9) \qquad h_0^{(1)}(k|\boldsymbol{r}-\boldsymbol{r}'|) = \sum_{|n|=0}^{\infty} \sum_{m=-n}^{n} M_{nm} h_n^{(1)}(kr_s) Y_n^m(\theta_s,\varphi_s),$$

and a j-expansion (local expansion) with respect to a (target) center $\boldsymbol{r}_c^t$:

$$(10) \qquad h_0^{(1)}(k|\boldsymbol{r}-\boldsymbol{r}'|) = \sum_{|n|=0}^{\infty} \sum_{m=-n}^{n} L_{nm} j_n(kr_t) Y_n^m(\theta_t,\varphi_t),$$

where

$$(11) \qquad M_{nm} = 4\pi j_n(kr_s') \overline{Y_n^m(\theta_s',\varphi_s')}, \quad L_{nm} = 4\pi h_n^{(1)}(kr_t') \overline{Y_n^m(\theta_t',\varphi_t')},$$
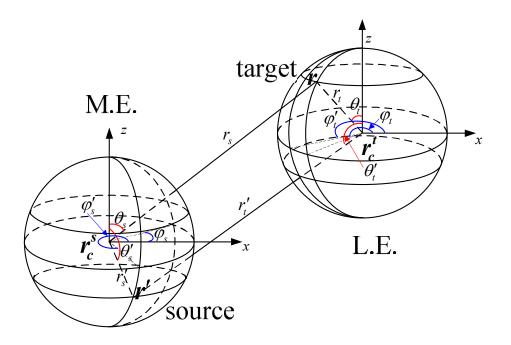
FIG. 1. *Spherical coordinates used in multipole and local expansions.*

$\boldsymbol{r}_c^s = (x_c^s, y_c^s, z_c^s)$ is the source center close to $\boldsymbol{r}'$, $\boldsymbol{r}_c^t = (x_c^t, y_c^t, z_c^t)$ is the target center close to $\boldsymbol{r}$, $(r_s, \theta_s, \varphi_s)$, $(r_t, \theta_t, \varphi_t)$ are the spherical coordinates of $\boldsymbol{r} - \boldsymbol{r}_c^s$ and $\boldsymbol{r} - \boldsymbol{r}_c^t$, respectively, and $(r_s', \theta_s', \varphi_s')$, $(r_t', \theta_t', \varphi_t')$ are the spherical coordinates of $\boldsymbol{r}' - \boldsymbol{r}_c^s$ and $\boldsymbol{r}' - \boldsymbol{r}_c^t$, respectively (Fig. 1).

Applying addition Theorem 3 to $h_n^{(1)}(kr_s)Y_n^m(\theta_s, \varphi_s)$ in (9), the translation from the h-expansion (9) to the j-expansion (10) is given by

$$(12) \qquad L_{nm} = \sum_{|\nu|=0}^{\infty} \sum_{\mu=-\nu}^{\nu} S_{n\nu}^{m\mu}(\boldsymbol{r}_c^t - \boldsymbol{r}_c^s)M_{\nu\mu}.$$

Similarly, we can shift the centers of h- and j-expansions via the following translations,

$$(13) \qquad \tilde{M}_{nm} = \sum_{\nu=0}^{\infty} \sum_{\mu=-\nu}^{\nu} \overline{\widehat{S}_{n\nu}^{m\mu}(\boldsymbol{r}_c^s - \tilde{\boldsymbol{r}}_c^s)}M_{\nu\mu}, \quad \tilde{L}_{nm} = \sum_{n=0}^{\infty} \sum_{\mu=-\nu}^{\nu} \widehat{S}_{\nu n}^{\mu m}(\tilde{\boldsymbol{r}}_c^t - \boldsymbol{r}_c^t)L_{\nu\mu},$$

where

$$(14) \qquad \tilde{M}_{nm} = 4\pi j_n(k\tilde{r}_s')\overline{Y_n^m(\tilde{\theta}_s', \tilde{\varphi}_s')}, \quad \tilde{L}_{nm} = 4\pi h_n^{(1)}(k\tilde{r}_t')\overline{Y_n^m(\tilde{\theta}_t', \tilde{\varphi}_t')}$$

are the h- and j-expansion coefficients at new centers $\tilde{\boldsymbol{r}}_c^s$ and $\tilde{\boldsymbol{r}}_c^t$, respectively.

An important feature in (9)-(10) is that the source and target coordinates are separated, which will be important in deriving low rank approximations for far fields in the FMM (cf. [16, 17]). However, this target-source separation can also be achieved in the Fourier spectral domain. A new derivation via Fourier domain for (9) and (10) will be given by using an integral representation of $h_0^{(1)}(k|\boldsymbol{r}|)$. Moreover, this approach can also be used to derive multipole and local expansions for the reaction components of Green's functions in layered media later.

2.2. A new derivation of h- and j-expansions. For a spherical wave, we have the well-known Sommerfeld identity

$$(15) \qquad h_0^{(1)}(k|\boldsymbol{r}|) = \frac{1}{2k\pi} \int_0^\infty \int_0^{2\pi} k_\rho e^{\mathrm{i}k_\rho(x\cos\alpha + y\sin\alpha)} \frac{e^{\mathrm{i}k_z|z|}}{k_z} d\alpha dk_\rho,$$

where $k_z = \sqrt{k^2 - k_\rho^2}$. It is necessary to point out that the identity (15) is for a lossless medium (i.e., k is real) and needs to be considered as a limiting case of a lossy medium. The contour for the integral of k_ρ is usually set by deforming the real axis to the fourth quadrant. In order to satisfy the outgoing wave radiation condition in the integrand, we have to ensure that $\mathfrak{Re}k_z > 0$ and $\mathfrak{Im}k_z > 0$. With the Sommerfeld identity (15), we can make a source-target separation in the spectral domain as follows

$$(16) \qquad \begin{aligned} h_0^{(1)}(k|\boldsymbol{r} - \boldsymbol{r}'|) &= \frac{1}{2k\pi} \int_0^\infty \int_0^{2\pi} k_\rho \frac{e^{\mathrm{i}\boldsymbol{k}\cdot(\boldsymbol{r}-\boldsymbol{r}_c^s)}e^{-\mathrm{i}\boldsymbol{k}\cdot(\boldsymbol{r}'-\boldsymbol{r}_c^s)}}{k_z} d\alpha dk_\rho, \\ h_0^{(1)}(k|\boldsymbol{r} - \boldsymbol{r}'|) &= \frac{1}{2k\pi} \int_0^\infty \int_0^{2\pi} k_\rho \frac{e^{\mathrm{i}\boldsymbol{k}\cdot(\boldsymbol{r}-\boldsymbol{r}_c^t)}e^{-\mathrm{i}\boldsymbol{k}\cdot(\boldsymbol{r}'-\boldsymbol{r}_c^t)}}{k_z} d\alpha dk_\rho \end{aligned}$$

for $z \geq z'$ where $\boldsymbol{k} = (k_\rho\cos\alpha, k_\rho\sin\alpha, k_z)$. Without loss of generality, here we only consider the case $z \geq z'$ for an illustration.

Next, we evoke the well-known Funk-Hecke formula [34, 24]

$$(17) \qquad \begin{aligned} e^{\mathrm{i}\boldsymbol{k}\cdot\boldsymbol{r}} &= \sum_{n=0}^\infty \sum_{m=-n}^n 4\pi\mathrm{i}^n j_n(kr)\overline{Y_n^m(\theta,\varphi)}\widehat{P}_n^m\left(\frac{k_z}{k}\right)e^{\mathrm{i}m\alpha} \\ &= \sum_{n=0}^\infty \sum_{m=-n}^n 4\pi\mathrm{i}^n j_n(kr)Y_n^m(\theta,\varphi)\widehat{P}_n^m\left(\frac{k_z}{k}\right)e^{-\mathrm{i}m\alpha}, \end{aligned}$$

which gives spherical harmonic expansions for plane waves and will be used for the plane waves inside (16). This classic Funk-Hecke formula only works for propagating plane wave, i.e., $0 < k_\rho \leq k$ where all components of the propagation vector $\boldsymbol{k}$ are real. However, the Fourier spectral representations (16) involve not only propagating but also evanescent plane waves, i.e., $k_\rho > k$ where k_z is purely imaginary. Therefore, for the spherical harmonic expansion of the evanescent plane wave, we need to extend the range of Funk-Hecke formula from $k_z \in \{\omega|0 \leq \omega \leq k\}$ to $k_z \in \{\omega|0 \leq \omega \leq k\} \cup \{\omega|\omega = \mathrm{i}y, y \geq 0\}$. Fortunately, we can show that formula (17) holds for all $k_z \in \mathbb{C}$ by choosing an appropriate branch for the square root function. To see this, the left hand side of (17) can be written as

$$(18) \qquad e^{\mathrm{i}\boldsymbol{k}\cdot\boldsymbol{r}} = e^{\mathrm{i}(\sqrt{k^2-k_z^2}(x\cos\alpha + y\sin\alpha) + k_z z)},$$

while the right hand side only has k_z as the argument of the normalized associated Legendre function. For the normalized associated Legendre function $\widehat{P}_n^m(x)$, we have $\widehat{P}_n^{-m}(x) = (-1)^m\widehat{P}_n^m(x), m > 0$ and also the Rodrigues' formula

$$(19) \qquad \widehat{P}_n^m(x) = \frac{1}{2^n n!}\sqrt{\frac{2n+1}{4\pi}\frac{(n-m)!}{(n+m)!}}(1-x^2)^{\frac{m}{2}}\frac{d^{n+m}}{dx^{n+m}}(x^2-1)^n.$$

If m is even, the analytic extension of $\widehat{P}_n^m(x)$ into the complex plane defined by

$$(20) \qquad \widehat{P}_n^m(z) = \frac{1}{2^n n!}\sqrt{\frac{2n+1}{4\pi}\frac{(n-m)!}{(n+m)!}}(1-z^2)^{\frac{m}{2}}\frac{d^{n+m}}{dz^{n+m}}(z^2-1)^n, \quad z \in \mathbb{C},$$

is a polynomial of z and hence is an entire function. For odd m, $\widehat{P}_n^m(x)$ can be written as

$$\widehat{P}_n^m(x) = \sqrt{1-x^2}Q_{n-1}(x), \tag{21}$$

where $Q_{n-1}(x)$ is a polynomial of at most $(n-1)$-th degree. Therefore, a complex extension defined by

$$\widehat{P}_n^m(z) = \sqrt{1-z^2}Q_{n-1}(z), \forall z \in \mathbb{C}, \tag{22}$$

involves the multivalued function $\sqrt{1-z^2}$ similarly as in (18). In order to have an analytic continuation for the Funk-Hecke formula (17) for complex k_z, we need to choose an appropriate branch in (18) and (22). Let us consider polar forms

$$z+1 = r_1 e^{i\theta_1}, \quad -\pi < \theta_1 \le \pi, \quad z-1 = r_2 e^{i\theta_2}, \quad -\pi < \theta_2 \le \pi,$$

where θ_1 and θ_2 are the principal values of the arguments of complex numbers $z+1$ and $z-1$. Then, we cut the complex plane from -1 to $+1$ along the real axis and choose the branch

$$\sqrt{1-z^2} = -i\sqrt{r_1 r_2}e^{i\frac{\theta_1+\theta_2}{2}}. \tag{23}$$

For any $x \in [-1,1]$, using this branch leads to

$$\lim_{\epsilon \to 0^+} \sqrt{1-(x+i\epsilon)^2} = \sqrt{1-x^2}, \quad \lim_{\epsilon \to 0^-} \sqrt{1-(x+i\epsilon)^2} = -\sqrt{1-x^2}. \tag{24}$$

The extensions $e^{i\boldsymbol{k}\cdot\boldsymbol{r}}$ and $\widehat{P}_n^m(z)$ defined by using (23) enjoy the same property, e.g.,

$$\lim_{\epsilon \to 0^+} \widehat{P}_n^m(x+i\epsilon) = \widehat{P}_n^m(x), \quad \lim_{\epsilon \to 0^-} \widehat{P}_n^m(x+i\epsilon) = -\widehat{P}_n^m(x), \quad \forall x \in [-1,1]. \tag{25}$$

We note that the extension of associated Legendre function also satisfies

$$\widehat{P}_n^m(-z) = (-1)^{n+m}\widehat{P}_n^m(z), \quad \widehat{P}_n^{-m}(z) = (-1)^m \widehat{P}_n^m(z), \tag{26}$$

and the recurrence formulas

$$\widehat{P}_0^0(z) = \frac{1}{4\pi}, \quad \widehat{P}_n^n(z) = -\sqrt{\frac{2n+1}{2n}}i\sqrt{r_1 r_2}e^{i\frac{\theta_1+\theta_2}{2}}\widehat{P}_{n-1}^{n-1}(z), \quad n = 1, 2, \cdots,$$
$$\widehat{P}_{m+k}^m(z) = a_{m+k}^m z\widehat{P}_{m+k-1}^m(z) - b_{m+k}^m\widehat{P}_{m+k-2}^m(z), \quad m = 0, 1, \cdots, \ k = 1, 2, \cdots, \tag{27}$$

where

$$a_n^m = \sqrt{\frac{(2n-1)(2n+1)}{(n-m)(n+m)}}, \quad b_n^m = \sqrt{\frac{(2n+1)(n-m-1)(n+m-1)}{(2n-3)(n+m)(n-m)}}.$$

The above recurrence formulas will be used in the implementation of the FMM.

Next, for the proof of the Funk-Hecke formula in the complex plane, we need the following lemmas.

LEMMA 4. *For any real number $a \ge 0$, there holds*

$$e^{iaz} = \sum_{n=0}^{\infty}(2n+1)i^n j_n(a)P_n(z), \quad \forall z \in \mathbb{C}, \tag{28}$$

where $j_n(a) = \sqrt{\frac{\pi}{2a}}J_{n+1/2}(a)$ is the spherical Bessel function of the first kind, $P_n(z)$ is the Legendre polynomial extended to the complex plane.

Proof. Recall the series (cf. [27, 10.60.7])

$$
(29) \qquad e^{\mathrm{i}a\cos\theta} = \sum_{n=0}^{\infty} (2n+1)\mathrm{i}^n j_n(a) P_n(\cos\theta),
$$

we can see that (28) holds for all $z \in [-1, 1]$. Next, we consider its extension to the whole complex plane. Apparently, $e^{\mathrm{i}az}$ is an entire function of z. Meanwhile, the spherical Bessel function $j_n(a)$ has the following upper bound (cf. [1, 9.1.62])

$$
(30) \qquad |j_n(a)| \le \frac{\Gamma(\frac{3}{2})}{\Gamma(n+\frac{3}{2})} \left(\frac{a}{2}\right)^n \le \frac{1}{n!}\left(\frac{a}{2}\right)^n.
$$

The Legendre polynomial $P_n(z)$ is a polynomial of degree n with n distinct roots $\{z_j\}_{j=1}^n$ in the interval $[-1, 1]$. Therefore,

$$
(31) \qquad |P_n(z)| = |a_n| \prod_{j=1}^{n} |z - z_j| \le 2^n (|z| + 1)^n, \quad \forall z \in \mathbb{C},
$$

here the estimate $a_n = \frac{(2n)!}{2^n (n!)^2} \le 2^n$ for the coefficient of z^n is used. These upper bounds for $j_n(a)$ and $P_n(z)$ give an estimate

$$
(32) \quad \sum_{n=0}^{\infty} (2n+1)|\mathrm{i}^n j_n(a) P_n(z)| \le \sum_{n=0}^{\infty} (2n+1)\frac{a^n(|z|+1)^n}{n!} = (2a(|z|+1)+1)e^{a(|z|+1)}.
$$

It is easy to show that the series on the righthand side of (28) converges uniformly in any compact set $D \subset \mathbb{C}$ and hence converges to an entire function of z. By the analytic extension theory, we have the proof. $\qquad\square$

By using the branch defined in (23) for the square roots, we have the extension of the well-known Legendre addition theorem [35, p.395].

LEMMA 5. *Let $\boldsymbol{w} = (\sqrt{1-w^2}\cos\alpha, \sqrt{1-w^2}\sin\alpha, w)$ be a vector with complex entries, θ, φ be the azimuthal angle and polar angles of a unit vector $\hat{\boldsymbol{r}}$. Define*

$$
(33) \qquad \beta(w) = w\cos\theta + \sqrt{1-w^2}\sin\theta\cos(\alpha-\varphi),
$$

then

$$
(34) \qquad P_n(\beta(w)) = \frac{4\pi}{2n+1} \sum_{m=-n}^{n} \widehat{P}_n^m(\cos\theta)\widehat{P}_n^m(w)e^{\mathrm{i}m(\alpha-\varphi)},
$$

for all $w \in \mathbb{C}$.

Proof. If $w \in [-1, 1]$ is real, we have $\beta(w) = \cos\langle \boldsymbol{w}, \hat{\boldsymbol{r}}\rangle$ and (34) is the well-known Legendre addition theorem. Define

$$
(35) \qquad g_n(w) = \frac{4\pi}{2n+1} \sum_{m=-n}^{n} \widehat{P}_n^m(\cos\theta)\widehat{P}_n^m(w)e^{\mathrm{i}m(\alpha-\varphi)}.
$$

By using the branch defined in (23) for the square roots in $\beta(w)$ and $\widehat{P}_n^m(w)$, $P_n(\beta(w))$ and $g_n(w)$ are extended to the complex plane. Moreover, they are analytic in $\mathbb{C}\backslash[-1, 1]$ and satisfy limit properties

$$
\lim_{\epsilon\to 0^+} P_n(\beta(x+\mathrm{i}\epsilon)) = P_n(\beta(x)), \quad \lim_{\epsilon\to 0^-} = P_n(\beta(x+\mathrm{i}\epsilon)) = -P_n(\beta(x)),
$$

$$
\lim_{\epsilon\to 0^+} g_n(x+\mathrm{i}\epsilon) = g_n(x), \quad \lim_{\epsilon\to 0^-} g_n(x+\mathrm{i}\epsilon) = -g_n(x)
$$

for all $x \in [-1, 1]$. That implies $P_n(\beta(w)) - g_n(w)$ takes angular boundary values zero on the set $[-1, 1]$ (taking limit from the upper complex plane). By using Luzin-Privalov theorem [11], we conclude that $P_n(\beta(w)) - g_n(w) = 0$ in $\mathbb{C} \setminus [-1, 1]$.   □

PROPOSITION 6. *Given* $\boldsymbol{r} = (x, y, z) \in \mathbb{R}^3$, $k > 0$, $\alpha \in [0, 2\pi)$ *and denoted by* (r, θ, φ) *the spherical coordinates of* $\boldsymbol{r}$, $\boldsymbol{k} = (\sqrt{k^2 - k_z^2} \cos \alpha, \sqrt{k^2 - k_z^2} \sin \alpha, k_z)$ *is a vector of complex entries. Choosing the branch* (23) *for* $\sqrt{k^2 - k_z^2}$ *in* $e^{i\boldsymbol{k}\cdot\boldsymbol{r}}$ *and* $\widehat{P}_n^m(\frac{k_z}{k})$, *then*

$$(36) \quad e^{i\boldsymbol{k}\cdot\boldsymbol{r}} = \sum_{n=0}^{\infty} \sum_{m=-n}^{n} \overline{A_n^m(\boldsymbol{r})} i^n \widehat{P}_n^m\left(\frac{k_z}{k}\right) e^{im\alpha} = \sum_{n=0}^{\infty} \sum_{m=-n}^{n} A_n^m(\boldsymbol{r}) i^n \widehat{P}_n^m\left(\frac{k_z}{k}\right) e^{-im\alpha},$$

holds for all $k_z \in \mathbb{C}$, *where*

$$A_n^m(\boldsymbol{r}) = 4\pi j_n(kr) Y_n^m(\theta, \varphi).$$

Proof. Define

$$\beta = \frac{k_z}{k} \cos \theta + \sqrt{1 - \frac{k_z^2}{k^2}} \sin \theta \cos(\alpha - \varphi),$$

then, $kr\beta = \boldsymbol{k} \cdot \boldsymbol{r}$. Let $a = kr$, $z = \beta$ in (28), we have

$$(37) \quad e^{i\boldsymbol{k}\cdot\boldsymbol{r}} = \sum_{n=0}^{\infty} (2n + 1) i^n j_n(kr) P_n(\beta).$$

Finally, the extension of Funk-Hecke formula (36) follows by applying Lemma 5.   □

To show the convergence rate of the expansion (36), we consider three different cases with $\boldsymbol{r} = (0.3, 0.4, z)$, $\alpha = \frac{\pi}{4}$. The convergence rates against p are depicted in Fig. 2 for the relative ℓ_2 error. Spectral convergence rates against p are observed while the expansion converges more slowly if one of $|\boldsymbol{k}|$, $|\boldsymbol{r}|$ and $|k_z|$ gets larger.

(a) $z = 0.5$, $k_z = 1 + i$ (b) $k = 1.8$, $k_z = 1 - 1.3i$ (c) $z = 0.5$, $k = 1.8$
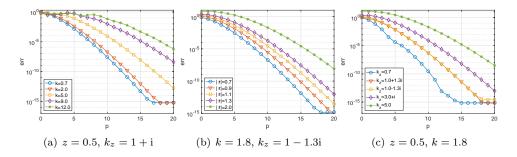
FIG. 2. *Convergence rate of the approximation using extended Funk-Hecke formula.*

Applying the spherical harmonic expansion (36) to exponential functions $e^{-i\boldsymbol{k}\cdot(\boldsymbol{r}'-\boldsymbol{r}_c^s)}$ and $e^{i\boldsymbol{k}\cdot(\boldsymbol{r}-\boldsymbol{r}_c^t)}$ in (16) gives

$$(38)$$

$$h_0^{(1)}(k|\boldsymbol{r} - \boldsymbol{r}'|) = \sum_{n=0}^{\infty} \sum_{m=-n}^{n} \frac{M_{nm}}{2k\pi} \int_0^{\infty} \int_0^{2\pi} k_\rho \frac{e^{i\boldsymbol{k}\cdot(\boldsymbol{r}-\boldsymbol{r}_c^s)}}{k_z} (-i)^n \widehat{P}_n^m\left(\frac{k_z}{k}\right) e^{im\alpha} d\alpha dk_\rho,$$

and

$$(39) \quad h_0^{(1)}(k|\boldsymbol{r} - \boldsymbol{r}'|) = \sum_{n=0}^{\infty} \sum_{m=-n}^{n} \hat{L}_{nm} j_n(kr_t) Y_n^m(\theta_t, \varphi_t),$$

for $z \geq z'$, where M_{nm} is defined in (11) and

$$(40) \qquad \hat{L}_{nm} = \frac{2\mathrm{i}^n}{k} \int_0^\infty \int_0^{2\pi} k_\rho \frac{e^{\mathrm{i}\boldsymbol{k}\cdot(\boldsymbol{r}_c^t - \boldsymbol{r}')}}{k_z} \widehat{P}_n^m\left(\frac{k_z}{k}\right) e^{-\mathrm{i}m\alpha} d\alpha dk_\rho.$$

For the convergence of the Sommerfeld-type integrals in the above expansions, we only consider centers such that their z-coordinates satisfy $z_c^s < z$ and $z_c^t > z'$. Recall the identity

$$(41) \qquad h_n^{(1)}(k|\boldsymbol{r}|)Y_n^m(\theta, \varphi) = \frac{1}{2k\pi} \int_0^\infty \int_0^{2\pi} k_\rho \frac{e^{\mathrm{i}\boldsymbol{k}\cdot\boldsymbol{r}}}{k_z}(-\mathrm{i})^n \widehat{P}_n^m\left(\frac{k_z}{k}\right) e^{\mathrm{i}m\alpha} d\alpha dk_\rho$$

for $z \geq 0$, we see that (38) and (39) are exactly the h-expansion (9) and j-expansion (10) for the case of $z \geq z'$.

To derive the translation from the h-expansion (38) to the j-expansion (39), we perform a further splitting in (38)

$$(42) \qquad e^{\mathrm{i}\boldsymbol{k}\cdot(\boldsymbol{r}-\boldsymbol{r}_c^s)} = e^{\mathrm{i}\boldsymbol{k}\cdot(\boldsymbol{r}-\boldsymbol{r}_c^t)} e^{\mathrm{i}\boldsymbol{k}\cdot(\boldsymbol{r}_c^t-\boldsymbol{r}_c^s)}$$

and apply expansion (36) to obtain the following translation

$$L_{nm} = \frac{2}{k} \sum_{\nu=0}^\infty \sum_{\mu=-\nu}^\nu M_{\nu\mu} \int_0^\infty \int_0^{2\pi} k_\rho \frac{e^{\mathrm{i}\boldsymbol{k}(\boldsymbol{r}_c^t-\boldsymbol{r}_c^s)}}{k_z}(-1)^\nu \mathrm{i}^{n+\nu} \widehat{P}_\nu^\mu\left(\frac{k_z}{k}\right) \widehat{P}_n^m\left(\frac{k_z}{k}\right) e^{\mathrm{i}(\mu-m)\alpha} d\alpha dk_\rho,$$

which implies an integral representation of $S_{n\nu}^{m\mu}(\boldsymbol{r}_c^t - \boldsymbol{r}_c^s)$ in (12). In order to ensure the convergence of the Sommerfeld-type integral in the translation operator, the z-coordinates of the centers are also assumed to satisfy $z_c^t > z_c^s$.

3. FMM for 3-D Helmholtz equation in layered media. In this section, the multipole and local expansions for the reaction components of layered media Green's function of 3-D Helmholtz equation will be derived by using the techniques introduced in the last section. Based on these expansions and relevant translation operators, FMM for 3-D Helmholtz Green's function in layered media can be developed.

3.1. Green's function of Helmholtz equation in layered media. Let us first review the integral representation of the layered Green's function derived in [32]. Consider a layered medium consisting of L interfaces located at $z = d_\ell, \ell = 0, 1, \cdots, L-1$ as shown in Fig. 3. A point source at $\boldsymbol{r}' = (x', y', z')$ is located in the ℓ'-th layer ($d_{\ell'} < z' < d_{\ell'-1}$). The layered Green's function for the Helmholtz equation satisfies

$$(43) \qquad \boldsymbol{\Delta}u(\boldsymbol{r}, \boldsymbol{r}') + k_\ell^2 u(\boldsymbol{r}, \boldsymbol{r}') = -\delta(\boldsymbol{r}, \boldsymbol{r}'),$$

at a field point $\boldsymbol{r} = (x, y, z)$ in the ℓ-th layer ($d_\ell < z < d_\ell - 1$) where $\delta(\boldsymbol{r}, \boldsymbol{r}')$ is the Dirac delta function and k_ℓ is the wave number in the ℓ-th layer. The system can be solved analytically in the Fourier (k_x, k_y)-domain for each layer in z by imposing transmission conditions at the interface between ℓ-th and $(\ell-1)$-th layer ($z = d_{\ell-1}$) as well as the decay conditions in the top and bottom-most layers as $z \to \pm\infty$ [8]. Inside a given layer, say, the ℓ-th layer, the solution has the form

$$(44) \qquad u(\boldsymbol{r}, \boldsymbol{r}') = \begin{cases} u_{\ell'\ell'}^{\mathrm{r}}(\boldsymbol{r}, \boldsymbol{r}') + \dfrac{e^{\mathrm{i}k_{\ell'}|\boldsymbol{r}-\boldsymbol{r}'|}}{4\pi|\boldsymbol{r}-\boldsymbol{r}'|}, & d_{\ell'} < z < d_{\ell'-1}, \\ u_{\ell\ell'}^{\mathrm{r}}(\boldsymbol{r}, \boldsymbol{r}'), & d_\ell < z < d_{\ell-1} \text{ and } \ell \neq \ell', \end{cases}$$
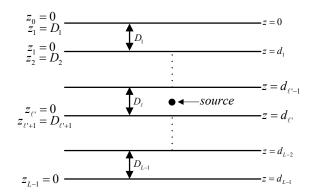
$z_0 = 0$
$z_1 = D_1$ ——————————————— $z = 0$

$z_1^r = 0$
$z_2^r = D_2$ ——————————————— $z = d_1$

———————————————— $z = d_{\ell'-1}$

$\quad D_\ell \quad$ ● ←—source

$z_{\ell'}^r = 0$
$z_{\ell'+1}^r = D_{\ell'+1}$ ——————————————— $z = d_{\ell'}$

———————————————— $z = d_{L-2}$

$z_{L-1}^r = 0$ ——————————————— $z = d_{L-1}$

FIG. 3. *Sketch of the layer structure for general multi-layer media.*

where

$$
(45) \qquad u_{\ell\ell'}^{\mathrm{r}}(\boldsymbol{r}, \boldsymbol{r}') = \begin{cases} u_{0\ell'}^{\uparrow}(\boldsymbol{r}, \boldsymbol{r}'), & \ell = 0, \\ u_{\ell\ell'}^{\uparrow}(\boldsymbol{r}, \boldsymbol{r}') + u_{\ell\ell'}^{\downarrow}(\boldsymbol{r}, \boldsymbol{r}'), & 0 < \ell < L, \\ u_{L\ell'}^{\downarrow}(\boldsymbol{r}, \boldsymbol{r}'), & \ell = L, \end{cases}
$$

is called the reaction field in the ℓ-th layer due to wave reflections and transmissions by the layered media. We can see that the reaction field $u_{\ell\ell'}^{\mathrm{r}}(\boldsymbol{r}, \boldsymbol{r}')$ has up-going and down-going components inside intermediate layers ($0 < \ell < L$). Only up-going or down-going component is required in the top- and bottom-most layers, respectively. The up- and down-going components have Sommerfeld integral representations

$$
(46) \quad \begin{aligned} u_{\ell\ell'}^{\uparrow}(\boldsymbol{r}, \boldsymbol{r}') &= \frac{\mathrm{i}}{8\pi^2} \int_0^\infty \int_0^{2\pi} k_\rho e^{\mathrm{i}\boldsymbol{k}_\alpha \cdot (\boldsymbol{\rho} - \boldsymbol{\rho}')} \frac{e^{\mathrm{i}k_{\ell z}(z - d_\ell)}}{k_{\ell z}} \psi_{\ell\ell'}^{\uparrow}(k_\rho, z') d\alpha dk_\rho, \quad \ell < L, \\ u_{\ell\ell'}^{\downarrow}(\boldsymbol{r}, \boldsymbol{r}') &= \frac{\mathrm{i}}{8\pi^2} \int_0^\infty \int_0^{2\pi} k_\rho e^{\mathrm{i}\boldsymbol{k}_\alpha \cdot (\boldsymbol{\rho} - \boldsymbol{\rho}')} \frac{e^{\mathrm{i}k_{\ell z}(d_{\ell-1} - z)}}{k_{\ell z}} \psi_{\ell\ell'}^{\downarrow}(k_\rho, z') d\alpha dk_\rho, \quad \ell > 0, \end{aligned}
$$

where $\boldsymbol{k}_\alpha = (k_\rho \cos \alpha, k_\rho \sin \alpha) = (k_x, k_y)$, $\boldsymbol{\rho} = (x, y)$, $\boldsymbol{\rho}' = (x', y')$, $k_{\ell z} = \sqrt{k_\ell^2 - k_\rho^2}$,

$$
(47) \quad \begin{cases} \psi_{\ell 0}^{\uparrow}(k_\rho, z') = e^{\mathrm{i}k_{0z}(z' - d_0)} \sigma_{\ell\ell'}^{\uparrow\uparrow}(k_\rho), \\[4pt] \psi_{\ell\ell'}^{\uparrow}(k_\rho, z') = e^{\mathrm{i}k_{\ell' z}(z' - d_{\ell'})} \sigma_{\ell\ell'}^{\uparrow\uparrow}(k_\rho) + e^{\mathrm{i}k_{\ell' z}(d_{\ell'-1} - z')} \sigma_{\ell\ell'}^{\uparrow\downarrow}(k_\rho), & 0 < \ell' < L, \\[4pt] \psi_{\ell\ell'}^{\downarrow}(k_\rho, z') = e^{\mathrm{i}k_{\ell' z}(z' - d_{\ell'})} \sigma_{\ell\ell'}^{\downarrow\uparrow}(k_\rho) + e^{\mathrm{i}k_{\ell' z}(d_{\ell'-1} - z')} \sigma_{\ell\ell'}^{\downarrow\downarrow}(k_\rho), & 0 < \ell' < L, \\[4pt] \psi_{\ell L}^{\downarrow}(k_\rho, z') = e^{\mathrm{i}k_{\ell' z}(d_{L-1} - z')} \sigma_{\ell L}^{\downarrow\downarrow}(k_\rho). \end{cases}
$$

The reaction densities $\sigma_{\ell\ell'}^{\uparrow\uparrow}(k_\rho), \sigma_{\ell\ell'}^{\uparrow\downarrow}(k_\rho), \sigma_{\ell\ell'}^{\downarrow\uparrow}(k_\rho), \sigma_{\ell\ell'}^{\downarrow\downarrow}(k_\rho)$ only depend on the layer structure and wave numbers. Equation (46)-(47) are general formulas which are applicable to multi-layered media. Here, we give explicit formulas for the reaction densities

of the three layers media with source in the middle layer, i.e.,

$$\sigma_{01}^{\uparrow\uparrow}(k_\rho) = \frac{k_1 k_{0z}(k_1 k_{1z} - k_2 k_{2z})e^{-\mathrm{i}d_1 k_{1z}}}{k_0 k_{0z}\kappa_{11} - \mathrm{i}k_1 k_{1z}\kappa_{12}}, \quad \sigma_{01}^{\uparrow\downarrow}(k_\rho) = \frac{k_1 k_{0z}k_1 k_{1z} + k_2 k_{2z}}{k_0 k_{0z}\kappa_{11} - \mathrm{i}k_1 k_{1z}\kappa_{12}},$$

$$\sigma_{11}^{\uparrow\uparrow}(k_\rho) = \frac{(k_1 k_{1z} - k_2 k_{2z})(k_1 k_{1z} + k_0 k_{0z})}{2(k_0 k_{0z}\kappa_{11} - \mathrm{i}k_1 k_{1z}\kappa_{12})}, \quad \sigma_{11}^{\downarrow\downarrow}(k_\rho) = \frac{(k_1 k_{1z} - k_0 k_{0z})(k_1 k_{1z} + k_2 k_{2z})}{2(k_0 k_{0z}\kappa_{11} - \mathrm{i}k_1 k_{1z}\kappa_{12})},$$

$$\sigma_{11}^{\uparrow\downarrow}(k_\rho) = \frac{k_1 k_{1z} - k_2 k_{2z}}{k_0 k_{0z}\kappa_{11} - \mathrm{i}k_1 k_{1z}\kappa_{12}} \frac{k_1 k_{1z} - k_0 k_{0z}}{2} e^{-\mathrm{i}d_1 k_{1z}},$$

$$\sigma_{11}^{\downarrow\uparrow}(k_\rho) = \frac{k_1 k_{1z} - k_0 k_{0z}}{k_0 k_{0z}\kappa_{11} - \mathrm{i}k_1 k_{1z}\kappa_{12}} \frac{k_1 k_{1z} - k_2 k_{2z}}{2} e^{-\mathrm{i}d_1 k_{1z}},$$

$$\sigma_{21}^{\downarrow\uparrow}(k_\rho) = \frac{k_1 k_{2z}(k_1 k_{1z} + k_0 k_{0z})}{k_0 k_{0z}\kappa_{11} - \mathrm{i}k_1 k_{1z}\kappa_{12}}, \quad \sigma_{21}^{\downarrow\downarrow}(k_\rho) = \frac{k_1 k_{2z}(k_1 k_{1z} - k_0 k_{0z})e^{-\mathrm{i}d_1 k_{1z}}}{k_0 k_{0z}\kappa_{11} - \mathrm{i}k_1 k_{1z}\kappa_{12}}.$$

where

$$\kappa_{11} = \frac{k_1 k_{1z} - k_2 k_{2z}}{2} e^{-2\mathrm{i}d_1 k_{1z}} + \frac{k_1 k_{1z} + k_2 k_{2z}}{2},$$

$$\kappa_{12} = \mathrm{i}\Big(\frac{k_2 k_{2z} - k_1 k_{1z}}{2} e^{-2\mathrm{i}d_1 k_{1z}} + \frac{k_1 k_{1z} + k_2 k_{2z}}{2} \Big).$$

Detailed derivation of the general formulas (45)-(47) and corresponding reaction densities for Green's function in layered media can be found in [32]. Although the density functions depend on the configuration of the layered media, they can be calculated at run time at any given point by solving one 2×2 linear system and multiplying the results by some 2×2 matrices.

3.2. Multipole and local expansions for general reaction component. Consider the reaction field in the middle layers, i.e.,

$$(48) \qquad u_{\ell\ell'}^{\mathrm{r}}(\boldsymbol{r}, \boldsymbol{r}') = u_{\ell\ell'}^{\uparrow}(\boldsymbol{r}, \boldsymbol{r}') + u_{\ell\ell'}^{\downarrow}(\boldsymbol{r}, \boldsymbol{r}').$$

Define

$$(49) \qquad \begin{aligned} \mathcal{E}_{\ell\ell'}^{\uparrow\uparrow}(\boldsymbol{r}, \boldsymbol{r}') &:= e^{\mathrm{i}\boldsymbol{k}_\alpha \cdot (\boldsymbol{\rho} - \boldsymbol{\rho}') + \mathrm{i}k_{\ell z}(z - d_\ell) + \mathrm{i}k_{\ell' z}(z' - d_{\ell'})}, \\ \mathcal{E}_{\ell\ell'}^{\uparrow\downarrow}(\boldsymbol{r}, \boldsymbol{r}') &:= e^{\mathrm{i}\boldsymbol{k}_\alpha \cdot (\boldsymbol{\rho} - \boldsymbol{\rho}') + \mathrm{i}k_{\ell z}(z - d_\ell) + \mathrm{i}k_{\ell' z}(d_{\ell' - 1} - z')}, \\ \mathcal{E}_{\ell\ell'}^{\downarrow\uparrow}(\boldsymbol{r}, \boldsymbol{r}') &:= e^{\mathrm{i}\boldsymbol{k}_\alpha \cdot (\boldsymbol{\rho} - \boldsymbol{\rho}') + \mathrm{i}k_{\ell z}(d_{\ell - 1} - z) + \mathrm{i}k_{\ell' z}(z' - d_{\ell'})}, \\ \mathcal{E}_{\ell\ell'}^{\downarrow\downarrow}(\boldsymbol{r}, \boldsymbol{r}') &:= e^{\mathrm{i}\boldsymbol{k}_\alpha \cdot (\boldsymbol{\rho} - \boldsymbol{\rho}') + \mathrm{i}k_{\ell z}(d_{\ell - 1} - z) + \mathrm{i}k_{\ell' z}(d_{\ell' - 1} - z')}. \end{aligned}$$

By expressions in (46) and (47) we have a further decomposition

$$(50) \qquad u_{\ell\ell'}^{\uparrow}(\boldsymbol{r}, \boldsymbol{r}') = u_{\ell\ell'}^{\uparrow\uparrow}(\boldsymbol{r}, \boldsymbol{r}') + u_{\ell\ell'}^{\uparrow\downarrow}(\boldsymbol{r}, \boldsymbol{r}'), \quad u_{\ell\ell'}^{\downarrow}(\boldsymbol{r}, \boldsymbol{r}') = u_{\ell\ell'}^{\downarrow\uparrow}(\boldsymbol{r}, \boldsymbol{r}') + u_{\ell\ell'}^{\downarrow\downarrow}(\boldsymbol{r}, \boldsymbol{r}'),$$

and each component has a Sommerfeld-type integral representation:

$$(51) \qquad u_{\ell\ell'}^{**}(\boldsymbol{r}, \boldsymbol{r}') = \frac{\mathrm{i}}{8\pi^2} \int_0^\infty \int_0^{2\pi} k_\rho \frac{\mathcal{E}_{\ell\ell'}^{**}(\boldsymbol{r}, \boldsymbol{r}')\sigma_{\ell\ell'}^{**}(k_\rho)}{k_{\ell z}} d\alpha dk_\rho.$$

Here and in the rest of this paper, $*$ stands for any one of arrows $\uparrow, \downarrow$, e.g., $u_{\ell\ell'}^{**}$ can be any of the four reaction components $u_{\ell\ell'}^{\uparrow\uparrow}, u_{\ell\ell'}^{\uparrow\downarrow}, u_{\ell\ell'}^{\downarrow\uparrow}, u_{\ell\ell'}^{\downarrow\downarrow}$. Note that the source and target coordinates are only involved in the exponential functions $\mathcal{E}_{\ell\ell'}^{**}(\boldsymbol{r}, \boldsymbol{r}')$. It is easy to make the following source-target separations

$$(52) \qquad \begin{aligned} \mathcal{E}_{\ell\ell'}^{*\uparrow}(\boldsymbol{r}, \boldsymbol{r}') &= \mathcal{E}_{\ell\ell'}^{*\uparrow}(\boldsymbol{r}, \boldsymbol{r}_c^s)e^{\mathrm{i}\boldsymbol{k}_\alpha \cdot (\boldsymbol{\rho}_c^s - \boldsymbol{\rho}') + \mathrm{i}k_{\ell' z}(z' - z_c^s)}, \\ \mathcal{E}_{\ell\ell'}^{*\downarrow}(\boldsymbol{r}, \boldsymbol{r}') &= \mathcal{E}_{\ell\ell'}^{*\downarrow}(\boldsymbol{r}, \boldsymbol{r}_c^s)e^{\mathrm{i}\boldsymbol{k}_\alpha \cdot (\boldsymbol{\rho}_c^s - \boldsymbol{\rho}') - \mathrm{i}k_{\ell' z}(z' - z_c^s)} \end{aligned}$$

by inserting the source center $\boldsymbol{r}_c^s$, and

(53)
$$\mathcal{E}_{\ell\ell'}^{\uparrow*}(\boldsymbol{r},\boldsymbol{r}') = \mathcal{E}_{\ell\ell'}^{\uparrow*}(\boldsymbol{r}_c^t,\boldsymbol{r}')e^{i\boldsymbol{k}_\alpha\cdot(\boldsymbol{\rho}-\boldsymbol{\rho}_c^t)+ik_{\ell z}(z-z_c^t)},$$
$$\mathcal{E}_{\ell\ell'}^{\downarrow*}(\boldsymbol{r},\boldsymbol{r}') = \mathcal{E}_{\ell\ell'}^{\downarrow*}(\boldsymbol{r}_c^t,\boldsymbol{r}')e^{i\boldsymbol{k}_\alpha\cdot(\boldsymbol{\rho}-\boldsymbol{\rho}_c^t)-ik_{\ell z}(z-z_c^t)}$$

by inserting the target center $\boldsymbol{r}_c^t$. Here $\boldsymbol{\rho}_c^s = (x_c^s, y_c^s)$, $\boldsymbol{\rho}_c^t = (x_c^t, y_c^t)$ are the x,y-coordinates of the centers $\boldsymbol{r}_c^s$ and $\boldsymbol{r}_c^t$. Moreover, Funk-Hecke formula (36) gives spherical harmonic expansions for the following plane waves:

$$e^{i\boldsymbol{k}_\alpha\cdot(\boldsymbol{\rho}_c^s-\boldsymbol{\rho}')\pm ik_{\ell'z}(z'-z_c^s)} = 4\pi\sum_{n=0}^{\infty}\sum_{m=-n}^{n}(-i)^n(\mp 1)^{n+m}j_n(k_{\ell'}r_s')\overline{Y_n^m(\theta_s',\varphi_s')}\widehat{P}_n^m\left(\frac{k_{\ell'z}}{k_{\ell'}}\right)e^{im\alpha},$$

$$e^{i\boldsymbol{k}_\alpha\cdot(\boldsymbol{\rho}-\boldsymbol{\rho}_c^t)\pm ik_{\ell z}(z-z_c^t)} = 4\pi\sum_{n=0}^{\infty}\sum_{m=-n}^{n}i^n(\pm 1)^{n+m}j_n(k_\ell r_t)Y_n^m(\theta_t,\varphi_t)\widehat{P}_n^m\left(\frac{k_{\ell z}}{k_\ell}\right)e^{-im\alpha},$$

where the fact that $Y_n^m(\pi-\theta,\varphi) = (-1)^{n+m}Y_n^m(\theta,\varphi)$ is used. Applying these expansions and source-target separation (52) and (53), we obtain

$$\mathcal{E}_{\ell\ell'}^{*\uparrow}(\boldsymbol{r},\boldsymbol{r}') = \mathcal{E}_{\ell\ell'}^{*\uparrow}(\boldsymbol{r},\boldsymbol{r}_c^s)\sum_{n=0}^{\infty}\sum_{m=-n}^{n}4\pi j_n(k_{\ell'}r_s')\overline{Y_n^m(\theta_s',\varphi_s')}(-1)^m i^n\widehat{P}_n^m\left(\frac{k_{\ell'z}}{k_{\ell'}}\right)e^{im\alpha},$$

$$\mathcal{E}_{\ell\ell'}^{*\downarrow}(\boldsymbol{r},\boldsymbol{r}') = \mathcal{E}_{\ell\ell'}^{*\downarrow}(\boldsymbol{r},\boldsymbol{r}_c^s)\sum_{n=0}^{\infty}\sum_{m=-n}^{n}4\pi j_n(k_{\ell'}r_s')\overline{Y_n^m(\theta_s',\varphi_s')}(-1)^n i^n\widehat{P}_n^m\left(\frac{k_{\ell'z}}{k_{\ell'}}\right)e^{im\alpha},$$

and

$$\mathcal{E}_{\ell\ell'}^{\uparrow*}(\boldsymbol{r},\boldsymbol{r}') = \mathcal{E}_{\ell\ell'}^{\uparrow*}(\boldsymbol{r}_c^t,\boldsymbol{r}')4\pi\sum_{n=0}^{\infty}\sum_{m=-n}^{n}j_n(k_\ell r_t)Y_n^m(\theta_t,\varphi_t)i^n\widehat{P}_n^m\left(\frac{k_{\ell z}}{k_\ell}\right)e^{-im\alpha},$$

$$\mathcal{E}_{\ell\ell'}^{\downarrow*}(\boldsymbol{r},\boldsymbol{r}') = \mathcal{E}_{\ell\ell'}^{\downarrow*}(\boldsymbol{r}_c^t,\boldsymbol{r}')4\pi\sum_{n=0}^{\infty}\sum_{m=-n}^{n}j_n(k_\ell r_t)Y_n^m(\theta_t,\varphi_t)(-1)^{n+m}i^n\widehat{P}_n^m\left(\frac{k_{\ell z}}{k_\ell}\right)e^{-im\alpha}.$$

Substituting the above identities into (51), we obtain the following multipole expansion:

(54) $$u_{\ell\ell'}^{**}(\boldsymbol{r},\boldsymbol{r}') = \sum_{n=0}^{\infty}\sum_{m=-n}^{n}M_{nm}\mathcal{F}_{nm}^{**}(\boldsymbol{r},\boldsymbol{r}_c^s), \quad M_{nm} = 4\pi j_n(k_{\ell'}r_s')\overline{Y_n^m(\theta_s',\varphi_s')},$$

with the expansion functions given by Sommerfeld-type integrals

(55)
$$\mathcal{F}_{nm}^{*\uparrow}(\boldsymbol{r},\boldsymbol{r}_c^s) = \frac{i}{8\pi^2}\int_0^{\infty}\int_0^{2\pi}k_\rho\frac{(-1)^m\mathcal{E}_{\ell\ell'}^{*\uparrow}(\boldsymbol{r},\boldsymbol{r}_c^s)\sigma_{\ell\ell'}^{*\uparrow}(k_\rho)}{k_{\ell z}}i^n\widehat{P}_n^m\left(\frac{k_{\ell'z}}{k_{\ell'}}\right)e^{im\alpha}d\alpha dk_\rho,$$

$$\mathcal{F}_{nm}^{*\downarrow}(\boldsymbol{r},\boldsymbol{r}_c^s) = \frac{i}{8\pi^2}\int_0^{\infty}\int_0^{2\pi}k_\rho\frac{(-1)^n\mathcal{E}_{\ell\ell'}^{*\downarrow}(\boldsymbol{r},\boldsymbol{r}_c^s)\sigma_{\ell\ell'}^{*\downarrow}(k_\rho)}{k_{\ell z}}i^n\widehat{P}_n^m\left(\frac{k_{\ell'z}}{k_{\ell'}}\right)e^{im\alpha}d\alpha dk_\rho.$$

It is worthy to point out that $\mathcal{F}_{nm}^{**}(\boldsymbol{r},\boldsymbol{r}_c^s)$ is only defined for $\boldsymbol{r}$ in the ℓ-th layer. Therefore, it could be seen as singular function for $\boldsymbol{r}$ outside the ℓ-th layer as reaction field produced by polarization charges there (more discussion on this issue will be given below). That is why we keep using the "multipole expansion" for expansion (54). Similarly, we obtain local expansion

(56) $$u_{\ell\ell'}^{**}(\boldsymbol{r},\boldsymbol{r}') = \sum_{n=0}^{\infty}\sum_{m=-n}^{n}L_{nm}^{**}j_n(k_\ell r_t)Y_n^m(\theta_t,\varphi_t),$$

with coefficients given by

$$(57) \quad \begin{aligned} L_{nm}^{\uparrow*} &= \frac{\mathrm{i}}{2\pi} \int_0^\infty \int_0^{2\pi} k_\rho \frac{\mathcal{E}_{\ell\ell'}^{\uparrow*}(\boldsymbol{r}_c^t, \boldsymbol{r}')\sigma_{\ell\ell'}^{\uparrow*}(k_\rho)}{k_{\ell z}} \mathrm{i}^n \widehat{P}_n^m\left(\frac{k_{\ell z}}{k_\ell}\right) e^{-\mathrm{i}m\alpha} d\alpha dk_\rho, \\ L_{nm}^{\downarrow*} &= \frac{(-1)^{n+m}\mathrm{i}}{2\pi} \int_0^\infty \int_0^{2\pi} k_\rho \frac{\mathcal{E}_{\ell\ell'}^{\downarrow*}(\boldsymbol{r}_c^t, \boldsymbol{r}')\sigma_{\ell\ell'}^{\downarrow*}(k_\rho)}{k_{\ell z}} \mathrm{i}^n \widehat{P}_n^m\left(\frac{k_{\ell z}}{k_\ell}\right) e^{-\mathrm{i}m\alpha} d\alpha dk_\rho. \end{aligned}$$

According to the definition of $\mathcal{E}_{\ell\ell'}^{**}(\boldsymbol{r}, \boldsymbol{r}_c^s)$ and $\mathcal{E}_{\ell\ell'}^{**}(\boldsymbol{r}_c^t, \boldsymbol{r}')$ in (49), the centers $\boldsymbol{r}_c^s$ and $\boldsymbol{r}_c^t$ have to satisfy

$$(58) \quad \begin{aligned} z_c^s > d_{\ell'}, \ z_c^t > d_\ell, &\quad \text{for } u_{\ell\ell'}^{\uparrow\uparrow}(\boldsymbol{r}, \boldsymbol{r}'); \quad z_c^s < d_{\ell'-1}, \ z_c^t < d_{\ell-1}, \quad \text{for } u_{\ell\ell'}^{\downarrow\downarrow}(\boldsymbol{r}, \boldsymbol{r}'); \\ z_c^s < d_{\ell'-1}, \ z_c^t > d_\ell, &\quad \text{for } u_{\ell\ell'}^{\uparrow\downarrow}(\boldsymbol{r}, \boldsymbol{r}'); \quad z_c^s > d_{\ell'}, \ z_c^t < d_{\ell-1}, \quad \text{for } u_{\ell\ell'}^{\downarrow\uparrow}(\boldsymbol{r}, \boldsymbol{r}') \end{aligned}$$

to ensure the exponential decay in $\mathcal{E}_{\ell\ell'}^{**}(\boldsymbol{r}, \boldsymbol{r}_c^s)$ and $\mathcal{E}_{\ell\ell'}^{**}(\boldsymbol{r}_c^t, \boldsymbol{r}')$ as $k_\rho \to \infty$ and hence the convergence of the corresponding Sommerfeld-type integrals in (55) and (57). These restriction can be met in practice, since we are considering targets in the ℓ-th layer and sources in the ℓ'-th layer.

3.3. Reaction components, associated equivalent polarization sources, and multipole and local expansions. It is well known that the h-expansion (9) and the j-expansion (10) for the free space Green's function have convergence rates of order $\mathcal{O}\left(\left(\frac{|\boldsymbol{r}'-\boldsymbol{r}_c^s|}{|\boldsymbol{r}-\boldsymbol{r}_c^s|}\right)^p\right)$ and $\mathcal{O}\left(\left(\frac{|\boldsymbol{r}-\boldsymbol{r}_c^t|}{|\boldsymbol{r}_c^t-\boldsymbol{r}'|}\right)^p\right)$, respectively. That is both multipole and local expansion converge exponentially as the target moving away from the source. These convergence results are the key for the success of the hierarchical tree structure design in FMM. However, multipole and local expansions (54)-(57) for reaction components have a different convergence behavior. According to the convergence analysis for multipole and local expansions of 2-D Green's function of Helmholtz equation in layered media (cf. [38]), we expect convergence estimates for the ME at $\boldsymbol{r}_c^s$ and the LE at $\boldsymbol{r}_c^t$ for the reaction components

$$(59) \quad \begin{aligned} \left| u_{\ell\ell'}^{**}(\boldsymbol{r}, \boldsymbol{r}') - \sum_{n=0}^p \sum_{m=-n}^n M_{nm}\mathcal{F}_{nm}^{**}(\boldsymbol{r}, \boldsymbol{r}_c^s) \right| &= \mathcal{O}\left(\left(\frac{|\boldsymbol{r}'-\boldsymbol{r}_c^s|}{d^{**}(\boldsymbol{r}, \boldsymbol{r}_c^s)}\right)^p\right), \\ \left| u_{\ell\ell'}^{**}(\boldsymbol{r}, \boldsymbol{r}') - \sum_{n=0}^p \sum_{m=-n}^n L_{nm}^{**} j_n(k_\ell r_t) Y_n^m(\theta_t, \varphi_t) \right| &= \mathcal{O}\left(\left(\frac{|\boldsymbol{r}-\boldsymbol{r}_c^t|}{d^{**}(\boldsymbol{r}_c^t, \boldsymbol{r}')}\right)^p\right), \end{aligned}$$

respectively, where

$$(60) \quad \begin{aligned} d^{\uparrow\uparrow}(\boldsymbol{r}, \boldsymbol{r}_c^s) &= \sqrt{(x-x_c^s)^2 + (y-y_c^s)^2 + (z-d_\ell + z_c^s - d_{\ell'})^2}, \\ d^{\uparrow\downarrow}(\boldsymbol{r}, \boldsymbol{r}_c^s) &= \sqrt{(x-x_c^s)^2 + (y-y_c^s)^2 + (z-d_\ell + d_{\ell'-1} - z_c^s)^2}, \\ d^{\downarrow\uparrow}(\boldsymbol{r}, \boldsymbol{r}_c^s) &= \sqrt{(x-x_c^s)^2 + (y-y_c^s)^2 + (d_{\ell-1} - z + z_c^s - d_{\ell'})^2}, \\ d^{\downarrow\downarrow}(\boldsymbol{r}, \boldsymbol{r}_c^s) &= \sqrt{(x-x_c^s)^2 + (y-y_c^s)^2 + (d_{\ell-1} - z + d_{\ell'-1} - z_c^s)^2}. \end{aligned}$$

Suppose $\boldsymbol{r}_c^s$ is a center close to source $\boldsymbol{r}'$ with a fixed distance $|\boldsymbol{r}'-\boldsymbol{r}_c^s|$, (59) indicates an important fact that the error of the truncated multipole expansion is not determined by the Euclidean distance between source center $\boldsymbol{r}_c^s$ and target $\boldsymbol{r}$ as in the free space case. Actually, the distances along z-direction have been replaced by summations of the distances between $\boldsymbol{r}$, $\boldsymbol{r}_c^s$ and corresponding nearest interfaces of the layered media. Similar conclusion can also be obtained for local expansion (56).

REMARK 3.1. *There are two special cases, i.e., $d^{\uparrow\downarrow}(\boldsymbol{r}, \boldsymbol{r}_c^s) = |\boldsymbol{r} - \boldsymbol{r}_c^s|$ if $\boldsymbol{r}$ and $\boldsymbol{r}_c^s$ are in the ℓ-th and $(\ell+1)$-th layer and $d^{\downarrow\uparrow}(\boldsymbol{r}, \boldsymbol{r}_c^s) = |\boldsymbol{r} - \boldsymbol{r}_c^s|$ if $\boldsymbol{r}$ and $\boldsymbol{r}_c^s$ are in the ℓ-th and $(\ell-1)$-th layer. Therefore, multipole and local expansions of $u_{\ell\ell+1}^{\uparrow\downarrow}(\boldsymbol{r}, \boldsymbol{r}_c^s)$ and $u_{\ell\ell-1}^{\downarrow\uparrow}(\boldsymbol{r}, \boldsymbol{r}_c^s)$ have the same convergence behavior as that of free space Green's function.*

We will give some numerical examples to show the convergence behavior of the multipole expansions in (59). Consider the multipole expansions of $u_{11}^{\uparrow\uparrow}$ and $u_{11}^{\uparrow\downarrow}$ in a three-layer media with $k_0 = 0.8$, $k_1 = 1.5$, $k_2 = 2.0$, $d_0 = 0, d_1 = -2.0$. In all the following examples, we fix $x = x' = 0.625$, $y = y' = 0.5$, $x_c^s = 1.0$, $y_c^s = 0.5$ for the coordinates of the target $\boldsymbol{r}$, source $\boldsymbol{r}'$ and source center $\boldsymbol{r}_c^s$, respectively. Moreover, we will have the distance $|\boldsymbol{r}' - \boldsymbol{r}_c^s| = 0.375$ fixed by keeping $z' = z_c^s$. For both components, we shall test three groups of z-coordinates given as follows

$$u_{11}^{\uparrow\uparrow} : z = z' = z_c^s = -1.8; \quad z = -1.8,\ z' = z_c^s = -1.0; \quad z = z' = z_c^s = -0.5;$$

$$u_{11}^{\uparrow\downarrow} : z = -1.8,\ z' = z_c^s = -0.2;\ z = -1.8,\ z' = z_c^s = -1.0;\ z = -0.5,\ z' = z_c^s = -1.5.$$

The relative errors against truncation number p are depicted in Fig. 4. We also use a linear polynomial to fit the value a in the expected exponential convergence $\mathcal{O}(a^p)$ via

$$\log err = p \log a + C.$$

The fitted values of a for all cases in Fig. 4 are given in the captions of the subfigures. The results clearly show that multipole expansion of u_{11}^{**} converges faster as the distance $d^{**}|\boldsymbol{r}, \boldsymbol{r}'|$ rather than Euclidean distance $|\boldsymbol{r} - \boldsymbol{r}'|$ increases. We also see that multipole expansion of $u_{11}^{\uparrow\downarrow}$ converges much faster than that of $u_{11}^{\uparrow\uparrow}$ as $d^{\uparrow\downarrow}(\boldsymbol{r}, \boldsymbol{r}_c^s) = d^{\uparrow\uparrow}(\boldsymbol{r}, \boldsymbol{r}_c^s)$. This can be explained by the extra exponential decay term inside the density $\sigma_{11}^{\uparrow\downarrow}(k_\rho)$, see Fig. 7.
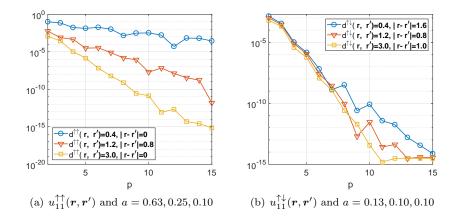

(a) $u_{11}^{\uparrow\uparrow}(\boldsymbol{r}, \boldsymbol{r}')$ and $a = 0.63, 0.25, 0.10$ (b) $u_{11}^{\uparrow\downarrow}(\boldsymbol{r}, \boldsymbol{r}')$ and $a = 0.13, 0.10, 0.10$

FIG. 4. *Errors of the multipole expansions vs. truncation order p.*

Polarization source for reaction field. In extending the FMM to the reaction field component of the layered Green's function, the hierarchical tree structure design as in free space FMM relies on using the Euclidean distance between source and target to determine either direct computation or multipole and local expansions are used for the computation of source-target interactions. Therefore, multipole and local expansions as given in (54)-(57) are generally not compatible with the hierarchical design of FMM. Considering the convergence behavior of ME in (59) and (60), we introduce
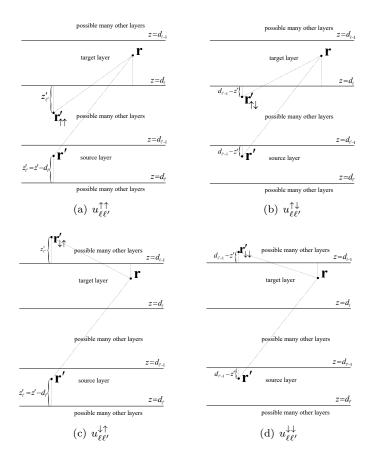
(a) $u_{\ell\ell'}^{\uparrow\uparrow}$ (b) $u_{\ell\ell'}^{\uparrow\downarrow}$

(c) $u_{\ell\ell'}^{\downarrow\uparrow}$ (d) $u_{\ell\ell'}^{\downarrow\downarrow}$

FIG. 5. *Location of equivalent polarization sources for the computation of $u_{\ell\ell'}^{**}$.*

equivalent polarization sources for the four types of reaction fields (see. Fig. 5)

$$
(61) \quad
\begin{aligned}
\boldsymbol{r}'_{\uparrow\uparrow} &= (x', y', d_\ell - (z' - d_{\ell'})), & \boldsymbol{r}'_{\uparrow\downarrow} &= (x', y', d_\ell - (d_{\ell'-1} - z')), \\
\boldsymbol{r}'_{\downarrow\uparrow} &= (x', y', d_{\ell-1} + (z' - d_{\ell'})), & \boldsymbol{r}'_{\downarrow\downarrow} &= (x', y', d_{\ell-1} + (d_{\ell'-1} - z'))
\end{aligned}
$$

which satisfy

$$
(62) \quad d^{\uparrow*}(\boldsymbol{r}, \boldsymbol{r}'_{\uparrow*}) = |\boldsymbol{r} - \boldsymbol{r}'_{\uparrow*}|, \quad \text{if } z > d_\ell; \quad d^{\downarrow*}(\boldsymbol{r}, \boldsymbol{r}'_{\downarrow*}) = |\boldsymbol{r} - \boldsymbol{r}'_{\downarrow*}|, \quad \text{if } z < d_{\ell-1}.
$$

Also, we define

$$
(63) \quad \widetilde{\mathcal{Z}}_{\ell\ell'}^{\uparrow}(z, z_s) := e^{\mathrm{i}k_{\ell z}(z-d_\ell)+\mathrm{i}k_{\ell' z}(d_\ell-z_s)}, \quad \widetilde{\mathcal{Z}}_{\ell\ell'}^{\downarrow}(z, z_s) := e^{\mathrm{i}k_{\ell z}(d_{\ell-1}-z)+\mathrm{i}k_{\ell' z}(z_s-d_{\ell-1})},
$$

and

$$
(64) \quad \widetilde{\mathcal{E}}_{\ell\ell'}^{*}(\boldsymbol{r}, \boldsymbol{r}_s) := e^{\mathrm{i}\boldsymbol{k}_\alpha \cdot (\boldsymbol{\rho}-\boldsymbol{\rho}_s)} \widetilde{\mathcal{Z}}_{\ell\ell'}^{*}(z, z_s).
$$

Recall the expressions (49), we can verify that

$$
(65) \quad \mathcal{E}_{\ell\ell'}^{\uparrow*}(\boldsymbol{r}, \boldsymbol{r}') = \widetilde{\mathcal{E}}_{\ell\ell'}^{\uparrow}(\boldsymbol{r}, \boldsymbol{r}'_{\uparrow*}), \quad \mathcal{E}_{\ell\ell'}^{\downarrow*}(\boldsymbol{r}, \boldsymbol{r}') = \widetilde{\mathcal{E}}_{\ell\ell'}^{\downarrow}(\boldsymbol{r}, \boldsymbol{r}'_{\downarrow*}).
$$

Therefore, the reaction components can be re-expressed using equivalent polarization sources as follows

(66)
$$u_{\ell\ell'}^{\uparrow*}(\boldsymbol{r},\boldsymbol{r}') = \tilde{u}_{\ell\ell'}^{\uparrow*}(\boldsymbol{r},\boldsymbol{r}'_{\uparrow*}) := \frac{\mathrm{i}}{8\pi^2}\int_0^\infty\int_0^{2\pi}k_\rho\frac{\widetilde{\mathcal{E}}_{\ell\ell'}^{\uparrow}(\boldsymbol{r},\boldsymbol{r}'_{\uparrow*})\sigma_{\ell\ell'}^{\uparrow*}(k_\rho)}{k_{\ell z}}d\alpha dk_\rho,$$

$$u_{\ell\ell'}^{\downarrow*}(\boldsymbol{r},\boldsymbol{r}') = \tilde{u}_{\ell\ell'}^{\downarrow*}(\boldsymbol{r},\boldsymbol{r}'_{\downarrow*}) := \frac{\mathrm{i}}{8\pi^2}\int_0^\infty\int_0^{2\pi}k_\rho\frac{\widetilde{\mathcal{E}}_{\ell\ell'}^{\downarrow}(\boldsymbol{r},\boldsymbol{r}'_{\downarrow*})\sigma_{\ell\ell'}^{\downarrow*}(k_\rho)}{k_{\ell z}}d\alpha dk_\rho.$$

Note that $\tilde{u}_{\ell\ell'}^{\uparrow*}$ and $\tilde{u}_{\ell\ell'}^{\downarrow*}$ have the same form as the two special cases $u_{\ell\ell+1}^{\uparrow\downarrow}$ and $u_{\ell\ell-1}^{\downarrow\uparrow}$, respectively, except for wave number $k_{\ell'z}$ and densities $\sigma_{\ell\ell'}^{**}$ in the ℓ'-th layer. Following the same derivation before, we obtain the following multipole expansion

(67) $$\tilde{u}_{\ell\ell'}^{**}(\boldsymbol{r},\boldsymbol{r}'_{**}) = \sum_{n=0}^\infty\sum_{m=-n}^n M_{nm}^{**}\widetilde{\mathcal{F}}_{nm}^{**}(\boldsymbol{r},\boldsymbol{r}_c^{**}), \quad M_{nm}^{**} = 4\pi j_n(k_{\ell'}r_s^{**})\overline{Y_n^m(\theta_s^{**},\varphi_s^{**})},$$

at equivalent polarization source centers $\boldsymbol{r}_c^{**}$ and local expansion

(68) $$\tilde{u}_{\ell\ell'}^{**}(\boldsymbol{r},\boldsymbol{r}'_{**}) = \sum_{n=0}^\infty\sum_{m=-n}^n L_{nm}^{**}j_n(k_\ell r_t)Y_n^m(\theta_t,\varphi_t)$$

at target center $\boldsymbol{r}_c^t$. Here, $(r_s^{**},\theta_s^{**},\varphi_s^{**})$ are spherical coordinates of $\boldsymbol{r}'_{**}-\boldsymbol{r}_c^{**}$, $\widetilde{\mathcal{F}}_{nm}^{**}(\boldsymbol{r},\boldsymbol{r}_c^{**})$ are represented by Sommerfeld-type integrals

(69)
$$\widetilde{\mathcal{F}}_{nm}^{\uparrow*}(\boldsymbol{r},\boldsymbol{r}_c^{\uparrow*}) = \frac{\mathrm{i}}{8\pi^2}\int_0^\infty\int_0^{2\pi}k_\rho\frac{\widetilde{\mathcal{E}}_{\ell\ell'}^{\uparrow}(\boldsymbol{r},\boldsymbol{r}_c^{\uparrow*})\sigma_{\ell\ell'}^{\uparrow*}(k_\rho)}{k_{\ell z}}(-\mathrm{i})^n\widehat{P}_n^m\left(\frac{k_{\ell'z}}{k_{\ell'}}\right)e^{\mathrm{i}m\alpha}d\alpha dk_\rho,$$

$$\widetilde{\mathcal{F}}_{nm}^{\downarrow*}(\boldsymbol{r},\boldsymbol{r}_c^{\downarrow*}) = \frac{\mathrm{i}}{8\pi^2}\int_0^\infty\int_0^{2\pi}k_\rho\frac{\widetilde{\mathcal{E}}_{\ell\ell'}^{\downarrow}(\boldsymbol{r},\boldsymbol{r}_c^{\downarrow*})\sigma_{\ell\ell'}^{\downarrow*}(k_\rho)}{k_{\ell z}}(-\mathrm{i})^n\widehat{P}_n^m\left(\frac{k_{\ell'z}}{k_{\ell'}}\right)e^{\mathrm{i}m\alpha}d\alpha dk_\rho,$$

and the local expansion coefficients are given by

(70)
$$L_{nm}^{\uparrow*} = \frac{\mathrm{i}}{2\pi}\int_0^\infty\int_0^{2\pi}k_\rho\frac{\widetilde{\mathcal{E}}_{\ell\ell'}^{\uparrow}(\boldsymbol{r}_c^t,\boldsymbol{r}'_{\uparrow*})\sigma_{\ell\ell'}^{\uparrow*}(k_\rho)}{k_{\ell z}}\mathrm{i}^n\widehat{P}_n^m\left(\frac{k_{\ell z}}{k_\ell}\right)e^{-\mathrm{i}m\alpha}d\alpha dk_\rho,$$

$$L_{nm}^{\downarrow*} = \frac{\mathrm{i}}{2\pi}\int_0^\infty\int_0^{2\pi}k_\rho\frac{(-1)^{n+m}\widetilde{\mathcal{E}}_{\ell\ell'}^{\downarrow}(\boldsymbol{r}_c^t,\boldsymbol{r}'_{\downarrow*})\sigma_{\ell\ell'}^{\uparrow*}(k_\rho)}{k_{\ell z}}\mathrm{i}^n\widehat{P}_n^m\left(\frac{k_{\ell z}}{k_\ell}\right)e^{-\mathrm{i}m\alpha}d\alpha dk_\rho.$$

Similar to the restrictions in (58), the centers $\boldsymbol{r}_c^{**}$ and $\boldsymbol{r}_c^t$ are required to satisfy

(71) $$z_c^{\uparrow*} < d_\ell, \quad z_c^{\downarrow*} > d_{\ell-1}, \quad z_c^t > d_\ell \text{ for } \tilde{u}_{\ell\ell'}^{\uparrow*}(\boldsymbol{r},\boldsymbol{r}'_{\uparrow*}); \quad z_c^t < d_{\ell-1} \text{ for } \tilde{u}_{\ell\ell'}^{\downarrow*}(\boldsymbol{r},\boldsymbol{r}'_{\downarrow*}).$$

Recall convergence results (59) and the fact (62), we conclude that ME (67) now satisfies

(72) $$\left|\tilde{u}_{\ell\ell'}^{**}(\boldsymbol{r},\boldsymbol{r}'_{**}) - \sum_{n=0}^p\sum_{m=-n}^n M_{nm}^{**}\widetilde{\mathcal{F}}_{nm}^{**}(\boldsymbol{r},\boldsymbol{r}_c^{**})\right| = \mathcal{O}\left(\left(\frac{|\boldsymbol{r}'_{**}-\boldsymbol{r}_c^{**}|}{|\boldsymbol{r}-\boldsymbol{r}_c^{**}|}\right)^p\right).$$

As a result, the Euclidean distance $|\boldsymbol{r}-\boldsymbol{r}'_{**}|$ can be used to determine if multipole expansions (67) are good approximations to the far reaction field. Similarly, the local expansion (68) for $\tilde{u}_{\ell\ell'}^{**}(\boldsymbol{r},\boldsymbol{r}'_{**})$ have a convergence of order $\mathcal{O}\left(\left(\frac{|\boldsymbol{r}-\boldsymbol{r}_c^t|}{|\boldsymbol{r}_c^t-\boldsymbol{r}'_{**}|}\right)^p\right)$. These

convergence results ensure that the hierarchical design can be applied in FMM with
kernels $\tilde{u}_{\ell\ell'}^{**}(\boldsymbol{r}, \boldsymbol{r}_{**}')$, ME (67) and LE (68).

Next, we discuss the center shifting and translation for ME (67) and LE (68). A
desirable feature of the expansions of reaction components discussed above is that the
formula (67) for the ME coefficients and the formula (68) for the LE have exactly the
same form as the formulas of h-expansion coefficients and j-expansion for free space
Green's function. Therefore, we can see that center shifting for multipole and local
expansions are exactly the same as free space case given in (13).

We only need to derive the translation operator from ME (67) to LE (68). Recall
the definition of exponential functions in (64), $\widetilde{\mathcal{E}}_{\ell\ell'}^{\uparrow}(\boldsymbol{r}, \boldsymbol{r}_c^{\uparrow*})$ and $\widetilde{\mathcal{E}}_{\ell\ell'}^{\downarrow}(\boldsymbol{r}, \boldsymbol{r}_c^{\downarrow*})$ have the
following splitting

$$\widetilde{\mathcal{E}}_{\ell\ell'}^{\uparrow}(\boldsymbol{r}, \boldsymbol{r}_c^{\uparrow*}) = \widetilde{\mathcal{E}}_{\ell\ell'}^{\uparrow}(\boldsymbol{r}_c^t, \boldsymbol{r}_c^{\uparrow*}) e^{i\boldsymbol{k}_\alpha \cdot (\boldsymbol{\rho} - \boldsymbol{\rho}_c^t)} e^{i k_{\ell z}(z - z_c^t)},$$

$$\widetilde{\mathcal{E}}_{\ell\ell'}^{\downarrow}(\boldsymbol{r}, \boldsymbol{r}_c^{\downarrow*}) = \widetilde{\mathcal{E}}_{\ell\ell'}^{\downarrow}(\boldsymbol{r}_c^t, \boldsymbol{r}_c^{\downarrow*}) e^{i\boldsymbol{k}_\alpha \cdot (\boldsymbol{\rho} - \boldsymbol{\rho}_c^t)} e^{-i k_{\ell z}(z - z_c^t)}.$$

Applying Funk-Hecke formula (36) again, we obtain

$$e^{i\boldsymbol{k}_\alpha \cdot (\boldsymbol{\rho} - \boldsymbol{\rho}_c^t)} e^{\pm i k_{\ell z}(z - z_c^t)} = 4\pi \sum_{n'=0}^{\infty} \sum_{|m'|=0}^{n'} i^{n'}(\pm 1)^\mu j_{n'}(k_\ell r_t) Y_{n'}^{m'}(\theta_t, \varphi_t) \widehat{P}_{n'}^{m'}\left(\frac{k_{\ell z}}{k_\ell}\right) e^{-im'\alpha},$$

where $\mu = (n' + m')(\text{mod } 2)$. Substituting into (67), the multipole expansion is
translated to local expansion (68) via

$$(73) \quad L_{nm}^{\uparrow*} = \sum_{n'=0}^{\infty} \sum_{|m'|=0}^{n'} T_{nm,n'm'}^{\uparrow*} M_{n'm'}^{\uparrow*}, \quad L_{nm}^{\downarrow*} = (-1)^{n+m} \sum_{n'=0}^{\infty} \sum_{|m'|=0}^{n'} T_{nm,n'm'}^{\downarrow*} M_{n'm'}^{\downarrow*},$$

and the multipole-to-local translation operators are given in integral forms as follows

$$
\begin{aligned}
(74) \quad & T_{nm,n'm'}^{\uparrow*} = \frac{(-1)^{n'}}{2\pi} \int_0^{\infty} \int_0^{2\pi} k_\rho \frac{\widetilde{\mathcal{E}}_{\ell\ell'}^{\uparrow}(\boldsymbol{r}_c^t, \boldsymbol{r}_c^{\uparrow*}) \sigma_{\ell\ell'}^{\uparrow*}(k_\rho)}{k_{\ell z}} Q_{nm}^{n'm'}(k_\rho) e^{i(m'-m)\alpha} d\alpha dk_\rho, \\
& T_{nm,n'm'}^{\downarrow*} = \frac{(-1)^{n'}}{2\pi} \int_0^{\infty} \int_0^{2\pi} k_\rho \frac{\widetilde{\mathcal{E}}_{\ell\ell'}^{\downarrow}(\boldsymbol{r}_c^t, \boldsymbol{r}_c^{\downarrow*}) \sigma_{\ell\ell'}^{\downarrow*}(k_\rho)}{k_{\ell z}} Q_{nm}^{n'm'}(k_\rho) e^{i(m'-m)\alpha} d\alpha dk_\rho,
\end{aligned}
$$

where

$$Q_{nm}^{n'm'}(k_\rho) = i^{n+n'+1} \widehat{P}_n^m\left(\frac{k_{\ell z}}{k_\ell}\right) \widehat{P}_{n'}^{m'}\left(\frac{k_{\ell' z}}{k_{\ell'}}\right).$$

We note that the convergence of the Sommerfeld-type integrals in (74) is ensured by
the conditions in (71).

REMARK 3.2. **Interpretation of Polarization Sources:** *In special situations
such as the half space (a two layer medium) with an impedance boundary condition
on the interface, the reaction fields can be expressed in terms of those from point and
line image charges located on the opposite side of the interface from the targets [9] [3].
However, in multilayered cases considered here, the reaction fields, given in terms of
complicated integral expressions, in general can not be expressed in terms of explicit
image charges. However, we can still introduce the polarization sources with locations
given in (61) and Fig. 5, which will represent the effect of the reaction fields and are
given locations based on the convergence behaviors of the MEs and LEs in (59) for
the corresponding reaction field components. For the practical FMM implementation
purpose, the locations of the polarization sources so defined enable us to decide whether*

the corresponding MEs can be used for the far field of the reaction components based on the distance between the far field location and the polarization sources, and thus, make the extension of FMMs to source interactions in layered media straightforward.

3.4. A FMM algorithm for sources in layered media. Let $\mathscr{P}_\ell = \{(Q_{\ell j}, \boldsymbol{r}_{\ell j}),$ $j = 1, 2, \cdots, N_\ell\}$ be a group of source particles distributed in the ℓ-th layer of a multi-layered medium with $L + 1$ layers (see Fig. 3). The interactions between all $N := N_0 + N_1 + \cdots + N_L$ particles are given by the summations

$$(75) \quad \Phi_\ell(\boldsymbol{r}_{\ell i}) = \Phi_\ell^{\text{free}}(\boldsymbol{r}_{\ell i}) + \sum_{\ell'=0}^{L-1} [\Phi_{\ell\ell'}^{\uparrow\uparrow}(\boldsymbol{r}_{\ell i}) + \Phi_{\ell\ell'}^{\downarrow\uparrow}(\boldsymbol{r}_{\ell i})] + \sum_{\ell'=1}^{L} [\Phi_{\ell\ell'}^{\uparrow\downarrow}(\boldsymbol{r}_{\ell i}) + \Phi_{\ell\ell'}^{\downarrow\downarrow}(\boldsymbol{r}_{\ell i})],$$

for $i = 1, 2, \cdots, N_\ell$, $\ell = 0, 1, \cdots, L$, where

$$(76) \quad \Phi_\ell^{\text{free}}(\boldsymbol{r}_{\ell i}) := \sum_{j=1, j \neq i}^{N_\ell} Q_{\ell j} h_0^{(1)}(k_\ell |\boldsymbol{r}_{\ell i} - \boldsymbol{r}_{\ell j}|), \quad \Phi_{\ell\ell'}^{**}(\boldsymbol{r}_{\ell i}) := \sum_{j=1}^{N_{\ell'}} Q_{\ell' j} u_{\ell\ell'}^{**}(\boldsymbol{r}_{\ell i}, \boldsymbol{r}_{\ell' j}).$$

Here, $u_{\ell\ell'}^{**}(\boldsymbol{r}, \boldsymbol{r}')$ are the reaction components of the layered Green's function in the ℓ-th layer due to a point source in the ℓ'-th layer. We omit the factor $\frac{ik_\ell}{4\pi}$ in $u_{\ell\ell'}^{**}(\boldsymbol{r}, \boldsymbol{r}')$ to maintain consistency with the spherical Hankel function used for the free space component. General formulas for $u_{\ell\ell'}^{**}(\boldsymbol{r}, \boldsymbol{r}')$ are given in (46)-(47).
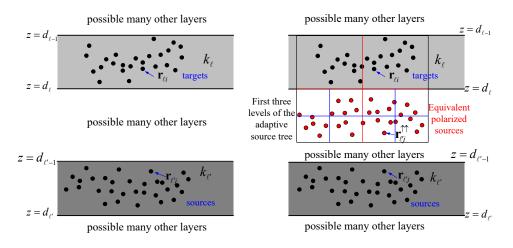

FIG. 6. *Equivalent polarization sources $\boldsymbol{r}_{\ell' j}^{\uparrow\uparrow}$ and boxes in source tree.*

Since the reaction components of Green's function in multi-layer media have different expressions (46) for source and target particles in different layers, it is necessary to perform calculation individually for interactions between any two groups of particles among the $L + 1$ groups $\{\mathscr{P}_\ell\}_{\ell=0}^L$. Here, we only consider the contribution from the reaction components and that from free space components will be calculated using free space FMM. Without loss of generality, let us focus on the computation of the $\uparrow\uparrow$ component in ℓ-th layer due to sources in ℓ'-th layer, i.e., $\Phi_{\ell\ell'}^{\uparrow\uparrow}(\boldsymbol{r}_{\ell i})$ for all $i = 1, 2, \cdots, N_\ell$ where we have source particles $\mathscr{P}_{\ell'}$ and target particles $\mathscr{P}_\ell$. According to the discussion in the last section, we use the equivalent polarization sources (see. Fig. 6)

$$\boldsymbol{r}_{\ell' j}^{\uparrow\uparrow} := (x_{\ell' j}, y_{\ell' j}, d_\ell - (z_{\ell' j} - d_{\ell'})),$$

and re-express $\Phi_{\ell\ell'}^{\uparrow\uparrow}(\boldsymbol{r}_{\ell i})$ as

$$(77) \qquad \Phi_{\ell\ell'}^{\uparrow\uparrow}(\boldsymbol{r}_{\ell i}) = \sum_{j=1}^{N_{\ell'}} Q_{\ell'j} \tilde{u}_{\ell\ell'}^{\uparrow\uparrow}(\boldsymbol{r}_{\ell i}, \boldsymbol{r}_{\ell'j}^{\uparrow\uparrow}), \quad i = 1, 2, \cdots, N_\ell.$$

A very important feature of the equivalent polarization sources $\{\boldsymbol{r}_{\ell'j}^{\uparrow\uparrow}\}_{j=1}^{N_{\ell'}}$ is that they are all separated from the corresponding targets $\{\boldsymbol{r}_{\ell i}\}_{i=1}^{N_\ell}$ by the interface $z = d_\ell$. As a matter of fact, they are located on different side of the interface $z = d_\ell$, see. Fig. 6 (right). Equivalent polarization sources (61) defined for other reaction components also have this property.

The framework of the free space FMM with ME (67), LE (68), M2L translation (73)-(74) and free space ME and LE center shifting allow us to use FMM for the computation of reaction component $\Phi_{\ell\ell'}^{\uparrow\uparrow}(\boldsymbol{r}_{\ell i})$. FMM for other reaction components can be treated in the same manner. In the FMM for reaction components, for each reaction component, a corresponding large box is defined to include all equivalent polarization sources and target particles where the adaptive tree structure will be built by a bisection procedure, see. Fig. 6 (right). Note that the validity of the ME (67), LE (68) and M2L translation (73) used in the algorithm imposes restrictions (71) on the centers, accordingly. This can be ensured by setting the largest box for the specific reaction component to be equally divided by the interface between equivalent polarization sources and targets, see. Fig. 6 (right). Thus, the largest box for the FMM implementation will be different for different reaction component. With this setting, all source and target boxes of level higher than zeroth level in the adaptive tree structure will have centers below or above the interface $z = d_\ell$, accordingly. The fast multipole algorithm for the computation of the reaction component $\Phi_{\ell\ell'}^{\uparrow\uparrow}(\boldsymbol{r}_{\ell i})$ is summarized in Algorithm 1. All the interaction given by (75) will be obtained by calculating all components and summing them up.

3.5. Implementation details for efficiency. In this section, we will discuss some implementation details regarding the computation of double integrals involved in the multipole and local expansions and multipole-to-local translations. Especially, they can be simplified by using the following identity

$$(78) \qquad J_n(z) = \frac{1}{2\pi \mathrm{i}^n} \int_0^{2\pi} e^{\mathrm{i}z\cos\theta + \mathrm{i}n\theta} d\theta.$$

In particular, multipole expansion functions in (69) can be simplified as

$$\widetilde{F}_{nm}^{\uparrow*}(\boldsymbol{r}, \boldsymbol{r}_c^{\uparrow*}) = \frac{(-\mathrm{i})^n \mathrm{i}^{m+1} e^{\mathrm{i}m\varphi_s^{\uparrow*}}}{4\pi} \int_0^\infty k_\rho J_m(k_\rho \rho_s^{\uparrow*}) \frac{\widetilde{\mathscr{Z}}_{\ell\ell'}^\uparrow(z, z_c^{\uparrow*}) \sigma_{\ell\ell'}^{\uparrow*}(k_\rho)}{k_{\ell z}} \widehat{P}_n^m \left(\frac{k_{\ell'z}}{k_{\ell'}}\right) dk_\rho,$$

$$\widetilde{F}_{nm}^{\downarrow*}(\boldsymbol{r}, \boldsymbol{r}_c^{\downarrow*}) = \frac{(-\mathrm{i})^n \mathrm{i}^{m+1} e^{\mathrm{i}m\varphi_s^{\downarrow*}}}{4\pi} \int_0^\infty k_\rho J_m(k_\rho \rho_s^{\downarrow*}) \frac{\widetilde{\mathscr{Z}}_{\ell\ell'}^\downarrow(z, z_c^{\downarrow*}) \sigma_{\ell\ell'}^{\downarrow*}(k_\rho)}{k_{\ell z}} \widehat{P}_n^m \left(\frac{k_{\ell'z}}{k_{\ell'}}\right) dk_\rho,$$

and the expression (70) for local expansion coefficients can be simplified as

$$L_{nm}^{\uparrow*} = (-1)^m \mathrm{i}^{n-m+1} e^{-\mathrm{i}m(\pi+\varphi_t^{\uparrow*})} \int_0^\infty k_\rho J_m(k_\rho \rho_t^{\uparrow*}) \frac{\widetilde{\mathscr{Z}}_{\ell\ell'}^\uparrow(z_c^t, z_{\uparrow*}') \sigma_{\ell\ell'}^{\uparrow*}(k_\rho)}{k_{\ell z}} \widehat{P}_n^m \left(\frac{k_{\ell z}}{k_\ell}\right) dk_\rho,$$

$$L_{nm}^{\downarrow*} = (-1)^n \mathrm{i}^{n-m+1} e^{-\mathrm{i}m(\pi+\varphi_t^{\downarrow*})} \int_0^\infty k_\rho J_m(k_\rho \rho_t^{\downarrow*}) \frac{\widetilde{\mathscr{Z}}_{\ell\ell'}^\downarrow(z_c^t, z_{\downarrow*}') \sigma_{\ell\ell'}^{\downarrow*}(k_\rho)}{k_{\ell z}} \widehat{P}_n^m \left(\frac{k_{\ell z}}{k_\ell}\right) dk_\rho,$$

Algorithm 1 FMM for general component $\Phi_{\ell\ell'}^{\uparrow\uparrow}(\boldsymbol{r}_{\ell i}), i = 1, 2, \cdots, N_\ell$

Determine z-coordinates of equivalent polarization sources for all source particles. Generate an adaptive hierarchical tree structure with polarization sources $\{Q_{\ell'j}, \boldsymbol{r}_{\ell'j}^{\uparrow\uparrow}\}_{j=1}^{N_{\ell'}}$, targets $\{\boldsymbol{r}_{\ell i}\}_{i=1}^{N_\ell}$ and pre-compute tables of $S_{nm,\nu\mu}^{\uparrow\uparrow}$ in (90).

Upward pass:

for $l = H \to 0$ **do**

    for all boxes j on source tree level l **do**

        if j is a leaf node **then**

            form the free-space ME using Eq. (67).

        else

            form the free-space ME by merging children's expansions using the free-space center shift translation operator (13).

        end if

    end for

end for

Downward pass:

for $l = 1 \to H$ **do**

    for all boxes j on target tree level l **do**

        shift the LE of j's parent to j itself using the free-space shifting (13).

        collect interaction list contribution using the source box to target box translation operator in Eq. (73) and (91) with pre-computed tables of $S_{nm,\nu\mu}^{\uparrow\uparrow}$.

    end for

end for

Evaluate Local Expansions:

for each leaf node (childless box) **do**

    evaluate the local expansion at each particle location.

end for

Local Direct Interactions:

for $i = 1 \to N$ **do**

    compute Eq. (77) of target particle i in the neighboring boxes using pre-computed tables of $S_{nm,\nu\mu}^{\uparrow\uparrow}$.

end for

---

where $(\rho_s^{**}, \varphi_s^{**})$ and $(\rho_t^{**}, \varphi_t^{**})$ are polar coordinates of $\boldsymbol{r}_{**}' - \boldsymbol{r}_c^{**}$ and $\boldsymbol{r}_{**}' - \boldsymbol{r}_c^t$ projected on xy plane. Moreover, the multipole to local translation (74) can be simplified as

$$
\text{(79)} \quad
\begin{aligned}
T_{nm,n'm'}^{\uparrow*} &= C_{n'mm'}^{\uparrow*} \int_0^\infty k_\rho J_{m'-m}(k_\rho \rho_{ts}^{\uparrow*}) \frac{\widetilde{\mathcal{Z}}_{\ell\ell'}^{\uparrow}(z_c^t, z_c^{\uparrow*}) \sigma_{\ell\ell'}^{\uparrow*}(k_\rho)}{k_{\ell z}} Q_{nm}^{n'm'}(k_\rho) dk_\rho, \\
T_{nm,n'm'}^{\downarrow*} &= C_{n'mm'}^{\downarrow*} \int_0^\infty k_\rho J_{m'-m}(k_\rho \rho_{ts}^{\downarrow*}) \frac{\widetilde{\mathcal{Z}}_{\ell\ell'}^{\downarrow}(z_c^t, z_c^{\downarrow*}) \sigma_{\ell\ell'}^{\downarrow*}(k_\rho)}{k_{\ell z}} Q_{nm}^{n'm'}(k_\rho) dk_\rho,
\end{aligned}
$$

where $C_{n'mm'}^{**} = (-1)^{n'} i^{m'-m} e^{i(m'-m)\varphi_{ts}^{**}}$ and $(\rho_{ts}^{**}, \varphi_{ts}^{**})$ is the polar coordinates of $\boldsymbol{r}_c^t - \boldsymbol{r}_c^{**}$ projected on xy plane. Denoting

$$
\text{(80)} \quad
\begin{aligned}
I_{nm,n'm'}^{\uparrow*}(\rho, z, z') &= \int_0^\infty k_\rho J_{m'-m}(k_\rho \rho) \frac{\widetilde{\mathcal{Z}}_{\ell\ell'}^*(z, z') \sigma_{\ell\ell'}^{\uparrow*}(k_\rho)}{k_{\ell z}} Q_{nm}^{n'm'}(k_\rho) dk_\rho, \\
I_{nm,n'm'}^{\downarrow*}(\rho, z, z') &= \int_0^\infty k_\rho J_{m'-m}(k_\rho \rho) \frac{\widetilde{\mathcal{Z}}_{\ell\ell'}^*(z, z') \sigma_{\ell\ell'}^{\downarrow*}(k_\rho)}{k_{\ell z}} Q_{nm}^{n'm'}(k_\rho) dk_\rho,
\end{aligned}
$$

then we have

$$
\widetilde{F}_{nm}^{**}(\boldsymbol{r}, \boldsymbol{r}_c^{**}) = \frac{(-1)^n \mathrm{i}^m e^{im\varphi_s^{**}}}{(\sqrt{4\pi})^3} I_{nm,00}^{**}(\rho_s^{**}, z, z_c^{**}),
$$

(81)
$$
L_{nm}^{\uparrow*} = \frac{\mathrm{i}^m e^{-im(\pi+\varphi_t^{\uparrow*})}}{\sqrt{4\pi}} I_{nm,00}^{\uparrow*}(\rho_t^{\uparrow*}, z_c^t, z_{\uparrow*}'),
$$

$$
L_{nm}^{\downarrow*} = \frac{(-1)^{n-m} \mathrm{i}^m e^{-im(\pi+\varphi_t^{\downarrow*})}}{\sqrt{4\pi}} I_{nm,00}^{\downarrow*}(\rho_t^{\downarrow*}, z_c^t, z_{\downarrow*}'),
$$

$$
T_{nm,n'm'}^{**} = C_{n'mm'}^{**} I_{nm,n'm'}^{*\uparrow}(\rho_{ts}^{**}, z_c^t, z_c^{**}).
$$

The FMM demands efficient computation of Sommerfeld-type integrals $I_{nm,n'm'}^{**}$ defined in (80). It is clear that they have oscillatory integrands with pole singularities in $\sigma_{\ell\ell'}^{**}(k_\rho)$ due to the existence of surface waves. For a long time, much effort has been made on the computation of this type of integrals, including using ideas from high-frequency asymptotics, rational approximation, contour deformation (cf. [3, 4, 8, 26, 29]), complex images (cf.[15, 29, 25, 2]), and methods based on special functions (cf. [20] or physical images (cf. [22, 23, 28, 21]). These integrals are convergent when the target and source particles are not exactly on the interfaces of a layered medium. Contour deformation with high order quadrature rules could be used for direct numerical computation at runtime. However, this becomes prohibitively expensive due to a large number of integrals needed in the FMM. In fact, $O(p^4)$ integrals will be required for each source box to target box translation. Moreover, the involved integrand decays more slowly as the order of the involved associated Legendre function increases. The length of contour needs to be very long to obtain a required accuracy.

Note that $I_{nm,n'm'}^{**}(\rho, z, z')$ is a smooth function with respect to (ρ, z, z'). It is feasible to make a pre-computed table on a fine grid and then use interpolation to obtain approximations for the integrals. If we make pre-computed tables for all $|m| \leq n, |m'| \leq n', n, n' = 0, 1, \cdots, p$, there will be $(p+1)^4$ 3-D tables to be stored. However, the number of pre-computed tables can be reduced to $4(p+1)(2p+1)$.

Let

(82)
$$
c_{nm} = \sqrt{\frac{2n+1}{4\pi} \frac{(n-m)!}{(n+m)!}}, \quad a_{nm}^j = \frac{(-1)^{n-j}(2j)! c_{nm}}{2^n j!(n-j)!(2j-n-m)!}.
$$

then

(83)
$$
\frac{c_{00}(x^2-1)^n}{2^n n!} = \sum_{k=0}^n a_{00}^j x^{2j}, \quad \frac{c_{nm}}{2^n n!} \frac{d^{n+m}}{dx^{n+m}}(x^2-1)^n = \sum_{j=\lceil \frac{n+m}{2} \rceil}^n a_{nm}^j x^{2j-n-m}.
$$

Recall the Rodrigues' formula

(84)
$$
\widehat{P}_n^m(x) = \frac{c_{nm}}{2^n n!}(1-x^2)^{\frac{m}{2}} \frac{d^{n+m}}{dx^{n+m}}(x^2-1)^n,
$$

for $0 \leq m \leq n$, and use the fact $k_{\ell z} = \sqrt{k_\ell^2 - k_\rho^2}$ and (83), we obtain

(85)
$$
\widehat{P}_n^m\left(\frac{k_{\ell z}}{k_\ell}\right) = \begin{cases} \displaystyle\sum_{s=0}^{n-r} b_{nm}^s \left(\frac{k_\rho}{k_\ell}\right)^{m+2s}, & n+m = 2r, \\ \displaystyle\frac{k_\ell}{k_{\ell z}} \sum_{s=0}^{n-r} b_{nm}^s \left(\frac{k_\rho}{k_\ell}\right)^{m+2s}, & n+m = 2r+1, \end{cases}
$$

where

$$(86) \qquad b_{nm}^s = \sum_{j=q}^{n} \frac{(-1)^s a_{nm}^j (j-r)!}{s!(j-r-s)!}, \quad q = \max\left(\left\lceil \frac{n+m}{2} \right\rceil, s+r\right).$$

Furthermore

$$(87) \qquad \widehat{P}_n^m\left(\frac{k_{\ell z}}{k_\ell}\right)\widehat{P}_{n'}^{m'}\left(\frac{k_{\ell' z}}{k_{\ell'}}\right) = \sum_{s=0}^{n-r+n'-r'} A_{nn'mm'}^s k_\rho^{m+m'+2s}\left(\frac{k_\ell}{k_{\ell z}}\right)^\mu \left(\frac{k_{\ell'}}{k_{\ell' z}}\right)^\nu,$$

where $\mu = (n+m)(\mathrm{mod}\ 2)$, $\nu = (n'+m')(\mathrm{mod}\ 2)$,

$$(88) \qquad A_{nn'mm'}^s = \sum_{t=\max(s-n'+r',0)}^{\min(s,n-r)} \frac{b_{nm}^t b_{n'm'}^{s-t}}{k_\ell^{m+2t} k_{\ell'}^{m'+2(s-t)}}.$$

For $-n \le m < 0$ or $-n' \le m' < 0$, similar formulas can be obtained by using the fact $\widehat{P}_n^m(z) = (-1)^m \widehat{P}_n^{-m}(z)$ for $m < 0$. In summary, we have

$$(89) \qquad \widehat{P}_n^m\left(\frac{k_{\ell z}}{k_\ell}\right)\widehat{P}_{n'}^{m'}\left(\frac{k_{\ell' z}}{k_{\ell'}}\right) = \sum_{s=0}^{n-r+n'-r'} A_{nn'mm'}^s k_\rho^{|m|+|m'|+2s}\left(\frac{k_\ell}{k_{\ell z}}\right)^\mu \left(\frac{k_{\ell'}}{k_{\ell' z}}\right)^\nu,$$

for all $n, n' = 0, 1, \cdots$, and $-n \le m \le n$, $-n' \le m' \le n'$ where $\mu = (n+|m|)(\mathrm{mod}\ 2)$, $\nu = (n'+|m'|)(\mathrm{mod}\ 2)$, $r = \lfloor (n+|m|)/2 \rfloor$, $r' = \lfloor (n'+|m'|)/2 \rfloor$, and

$$A_{nn'mm'}^s = \sum_{t=\max(s-n'+r',0)}^{\min(s,n-r)} \frac{\tau_m \tau_{m'} b_{n|m|}^t b_{n'|m'|}^{s-t}}{k_\ell^{|m|+2t} k_{\ell'}^{|m'|+2(s-t)}}, \quad \tau_\nu = \begin{cases} 1, & \nu \ge 0, \\ (-1)^{-\nu}, & \nu < 0. \end{cases}$$

Here, we also use the notation $A_{nn'mm'}^s$ since it is equal to the coefficients defined in (88) for $m, m' \ge 0$. Define integrals

$$(90) \qquad \begin{aligned} \mathcal{S}_{nm,ij}^{\uparrow*}(\rho, z, z') &= \int_0^\infty k_\rho^{m+1} J_n(k_\rho \rho) \frac{\widetilde{\mathcal{Z}}_{\ell\ell'}^{\uparrow}(z,z') \sigma_{\ell\ell'}^{\uparrow*}(k_\rho)}{k_{\ell z}} \left(\frac{k_\ell}{k_{\ell z}}\right)^i \left(\frac{k_{\ell'}}{k_{\ell' z}}\right)^j dk_\rho, \\ \mathcal{S}_{nm,ij}^{\downarrow*}(\rho, z, z') &= \int_0^\infty k_\rho^{m+1} J_n(k_\rho \rho) \frac{\widetilde{\mathcal{Z}}_{\ell\ell'}^{\downarrow}(z,z') \sigma_{\ell\ell'}^{\downarrow*}(k_\rho)}{k_{\ell z}} \left(\frac{k_\ell}{k_{\ell z}}\right)^i \left(\frac{k_{\ell'}}{k_{\ell' z}}\right)^j dk_\rho. \end{aligned}$$

Then

$$(91) \qquad I_{nm,n'm'}^{**}(\rho, z, z') = \mathrm{i}^{n+n'+1} \sum_{s=0}^{n-r+n'-r'} A_{nn'mm'}^s \mathcal{S}_{m-m',|m|+|m'|+2s,\mu\nu}^{**}(\rho, z, z'),$$

where $\mu = (n+|m|)(\mathrm{mod}\ 2)$, $\nu = (n'+|m'|)(\mathrm{mod}\ 2)$. We pre-compute integrals $\mathcal{S}_{nm,\mu\nu}^{**}(\rho, z, z')$ on a 3-D grid $\{\rho_i, z_j, z_k'\}$ in the domain of interest for all $n = 0, 1, \cdots, p$; $m = 0, 1, \cdots, 2n+1$; $\mu, \nu = 0, 1$. Then, a polynomial interpolation is performed for the computation of integrals in the FMM.

To compute Sommerfeld-type integrals $\mathcal{S}_{nm,\mu\nu}^{**}(\rho, z, z')$, it is typical to deform the integration contour by pushing it away from the real line into the fourth quadrant of the complex k_ρ-plane to avoid branch points and poles in the integrand, see Fig. 7. Here, we use a piecewise smooth contour which consists of two segments:

$$(92) \qquad \Gamma_1: \{k_\rho = \mathrm{i}t, -b \le t \le 0\}, \quad \Gamma_2: \{k_\rho = t - \mathrm{i}b, \ 0 \le t < \infty\}.$$

We truncate Γ_2 at a point $t_{max} > 0$, where the integrand has decayed to a user specified tolerance. As an example, we plot the density $\sigma_{11}^{**}(k_\rho)$ along Γ_2 (see, Fig. 7 (c)). The three layers case with $k_0 = 1.5, k_1 = 0.8, k_2 = 2.0, d_0 = 0, d_1 = -2.0$ and density given in Section 3 is used. We can see that the density $\sigma_{11}^{**}(k_\rho)$ is bounded.
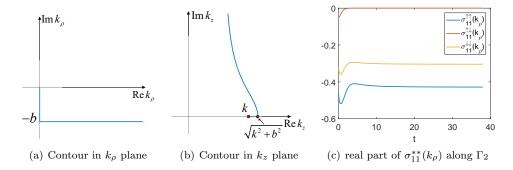
(a) Contour in k_ρ plane   (b) Contour in k_z plane   (c) real part of $\sigma_{11}^{**}(k_\rho)$ along Γ_2

FIG. 7. *Deformed contour for the computation of Sommerfeld-type integrals.*

4. Numerical results. In this section, we present numerical results to demonstrate the performance of the proposed FMM for time harmonic wave scattering in layered media. This algorithm is implemented based on an open-source adaptive FMM package DASHMM [14] on a workstation with two Xeon E5-2699 v4 2.2 GHz processors (each has 22 cores) and 500GB RAM using the gcc compiler version 6.3.

We test the problem in three layers media with interfaces placed at $z_0 = 0$, $z_1 = -1.2$. Particles are set to be uniformly distributed in irregular domains which are obtained by shifting the domain determined by $r = 0.5 - a + \frac{a}{8}(35\cos^4\theta - 30\cos^2\theta + 3)$ with $a = 0.1, 0.15, 0.05$ to new centers $(0, 0, 0.6)$, $(0, 0, -0.6)$ and $(0, 0, -1.8)$, respectively (see Fig. 8 (a) for the cross section of the domains). All particles are generated by keeping the uniform distributed particles in a larger cube within corresponding irregular domains. In the layered media, the wave numbers are $k_0 = 1.2$, $k_1 = 1.5$, $k_2 = 1.8$. Let $\widetilde{\Phi}_\ell(\boldsymbol{r}_{\ell i})$ be the approximated values of $\Phi_\ell(\boldsymbol{r}_{\ell i})$ calculated by FMM. For accuracy test, we put $N = 912 + 640 + 1296$ particles in the irregular domains in three layers see Fig. 8 (a). Convergence rates for the relative ℓ^2 error (Err_2) and relative maximum error (Err_{max}) against p are depicted in Fig. 8 (b). The CPU time for the computation of all three free space components $\{\Phi_\ell^{free}(\boldsymbol{r}_{\ell i})\}_{\ell=0}^2$, three selected reaction components $\{\Phi_{00}^{\uparrow\uparrow}, \Phi_{11}^{\uparrow\uparrow}, \Phi_{22}^{\downarrow\downarrow}\}$ and all sixteen reaction components $\Phi_{\ell\ell'}^{**}(\boldsymbol{r}_{\ell i})$ with truncation $p = 4$ are compared in Fig. 8 (c) for up to 3 millions particles. It shows that all of them have an $O(N)$ complexity while the CPU time for the computation of reaction components has a much smaller linear scaling constant due to the fact that most of the equivalent polarization sources are well-separated with the targets. CPU time with multiple cores is given in Table 1 and it shows that, due to the small amount of CPU time in computing the reaction components, the speedup of the parallel computing is mainly decided by the computation of the free space components. Here, we only use parallel implementation within the computation of each component, and all reaction components are computed independently. Therefore, it is straightforward to implement a version of the code which computes all components in parallel.

Pre-computed translation operator tables: Given the truncation order p, there will be $4(p+1)(2p+1)$ 3-D tables to be pre-computed, whose size depends on the required accuracy. In our numerical tests, we use tables with $30 \times 30 \times 30$ mesh with an interpolation polynomial of order 3. Then, each table have 91^3 integrals to be calculated. For each integral, the infinite interval is truncated at $t_{max} = 100$ and a mesh with 51 sub-intervals and 30 Gaussian quadrature points in each sub-interval is used. It takes about 8.5 seconds on our workstation to compute one 3-D table as

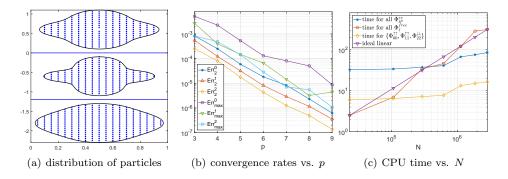all the integrals can be calculated in parallel.

(a) distribution of particles   (b) convergence rates vs. p (c) CPU time vs. N

FIG. 8. *Performance of FMM for a three layers media problem.*

cores	N	time for all $\{\Phi_\ell^{free}\}_{\ell=0}^2$	time for $\{\Phi_{00}^{\uparrow\uparrow}, \Phi_{11}^{\uparrow\uparrow}, \Phi_{22}^{\downarrow\downarrow}\}$
1	618256	46.01	4.60
	1128556	120.9	12.13
	1862568	282.4	13.88
	2861288	306.9	15.22
6	618256	8.75	2.77
	1128556	21.95	4.00
	1862568	52.19	4.57
	2861288	57.04	5.15
36	618256	2.29	2.74
	1128556	5.00	3.21
	1862568	11.45	3.59
	2861288	12.60	3.90

TABLE 1
Comparison of CPU time with multiple cores ($p = 4$).

5. Conclusion and discussion. In this paper, we presented an $O(N)$ fast multipole method for the calculation of the discretized integral operator for the low-frequency Helmholtz equation in 3-D layered media. The layered media Green's function is decomposed into a free space and four types of reaction field component(s). Using the spectral form of the layered Green's functions and the Funk-Hecke identity, we developed new multipole expansion of $O(p^2)$ terms for the far field of the reaction components, which can be associated with polarization sources at specific locations for the reaction field components. Multipole to local translation operators are also developed for the reaction fields. As a result, the traditional ME-based FMM can be applied to both the free space part and the reaction fields once the polarization sources are combined with the original sources. Due to the separation of the polarization and the original source charges by a material interface, the computational cost from the reaction field parts is only a fraction of that of the FMM for the free space part. For a given layered structure, besides the one time pre-computations of interpolation tables for the translation operator, computing the wave interactions of many sources in layered media costs the same as that for the wave interactions in the free space.

The complexity of the FMM on L for a $L-$layer medium will scale as $O(L^2)$ as the reaction component expression is different for different combination of source

and target layers, the source-target interactions will need to be computed, separately. However, the FMMs for different group of reaction components can be done in parallel, and in practice L is usually on the order of 10. Also, to reduce the pre-computation time of the tables for the M2L translation matrices, which involve the Sommerfeld integrals (90) with smooth integrands along the deformed contour, faster algorithms can be developed by using better quadrature rule (e.g., Clenshaw-Curtis-Filon-type method) and the recurrence formula of Bessel functions (see details in [39]).

The FMM developed here only considered low-frequency Helmholtz equations. Similar to the free space case, the multipole-expansion based FMM in this paper can not handle high frequency wave source interactions well as the number of terms in the MEs will increase in proportion to $k * D$ [12] where k is the wave number and D is the size of the scatterer. To address this difficulty, plane waves expansions could be introduced to yield diagonal forms for the translation operators in the FMM to produce an $O(N \log N)$ fast algorithm [30][7]. Though, the plane wave expansion may suffer a low-frequency breakdown when interaction between sources within sub-wavelength distance is computed for large objects with small fine structures. Therefore, it is important to develop a stable FMM applicable to a broad range of frequencies from low to high wave numbers without the low-frequency break down while still applicable to high frequency scattering. Various methods have been proposed toward this goal again for the free space case, including hybrid approaches combining multipole and plane wave expansions [5][36] as well as FMMs using stable plane wave expansions [13] and inhomogeneous plane waves [19].

As a future work, as the Green's functions for the layered media are given in terms of plane waves via Sommerfeld integration, we will study broadband FMMs for the layered media. For an immediate task, we shall carry out error analysis for the new MEs and M2L operators for the reaction components for the Helmholtz equations in 3-D layered media, extending our results for the 2-D Helmholtz equations [38].

REFERENCES

[1] M. Abramowitz and I. Stegun. *Handbook of Mathematical Functions*. Dover, New York, 1964.
[2] A. Alparslan, M. I. Aksun, and K. A. Michalski. Closed-form Green's functions in planar layered media for all ranges and materials. IEEE Trans. MTT, 58(3):602–613, 2010.
[3] W. Cai. *Computational Methods for Electromagnetic Phenomena: electrostatics in solvation, scattering, and electron transport.* Cambridge University Press, New York, NY, 2013.
[4] W. Cai and T. J. Yu. Fast calculations of dyadic Green's functions for electromagnetic scattering in a multilayered medium. J. Comput. Phys., 165(1):1–21, 2000.
[5] H. Cheng, W.Y. Crutchfield, Z. Gimbutas, L. F. Greengard, J. F. Ethridge, J. Huang, V. Rokhlin, N. Yarvin, J. Zhao, A wideband fast multipole method for the Helmholtz equation in three dimensions. J. Computat. Phys.. 2006 Jul 20;216(1):300-25.
[6] W. C. Chew. Recurrence relations for three-dimensional scalar addition theorem. J. Electromagnet. Waves Appl., 6(1-4):133–142, 1992.
[7] W. C. Chew, S. Koc, J. M. Song, C. C. Lu, E. Michielssen, A succinct way to diagonalize the translation matrix in three dimensions. Microw. Opt. Techn. Let. 1997 Jun 20;15(3):144-7.
[8] M. H. Cho and W. Cai. A parallel fast algorithm for computing the Helmholtz integral operator in 3-D layered media. J. Comput. Phys., 231(17):5910–5925, 2012.
[9] M. H. Cho, J. F. Huang, D. X. Chen, and W. Cai. A heterogeneous FMM for layered media Helmholtz equation I: Two layers in $\mathbb{R}^2$. J. Comput. Phys., 369:237–251, 2018.
[10] B. A. Cipra. The best of the 20th century: Editors name top 10 algorithms. SIAM news, 33(4):1–2, 2000.
[11] E. F. Collingwood and A. J. Lohwater. *The theory of cluster sets*, volume 56. Cambridge University Press, 2004.
[12] E. Darve, The fast multipole method I: error analysis and asymptotic complexity. SIAM J.

Numer. Anal.. 2000;38(1):98-128.

[13] E. Darve, P. Hav, A fast multipole method for Maxwell equations stable at all frequencies. Philosophical Transactions of the Royal Society of London. Series A: Mathematical, Physical and Engineering Sciences. 2004 Jan 29;362(1816):603-28.

[14] J. DeBuhr, B. Zhang, A. Tsueda, V. Tilstra-Smith, and T. Sterling. Dashmm: Dynamic adaptive system for hierarchical multipole methods. Commun. Comput. Phys., 20(4):1106–1126, 2016.

[15] D. G. Fang, J. J. Yang, and G. Y. Delisle. Discrete image theory for horizontal electric dipoles in a multilayered medium. In IEE Proc. H. Microw. Antennas Propag., volume 135, pages 297–303. IET, 1988.

[16] L. Greengard and V. Rokhlin. A fast algorithm for particle simulations. J. Comput. phys., 73(2):325–348, 1987.

[17] L. Greengard and V. Rokhlin. A new version of the fast multipole method for the Laplace equation in three dimensions. Acta Numer., 6:229–269, 1997.

[18] N. A Gumerov and R. Duraiswami. Recursions for the computation of multipole translation and rotation coefficients for the 3-D Helmholtz equation. SIAM J. Sci. Comput., 25(4):1344–1381, 2004.

[19] B. Hu, W. C. Chew, Fast inhomogeneous plane wave algorithm for electromagnetic solutions in layered medium structures: two-dimensional case, Radio Sci. 35 (1) (2000) 31–43.

[20] I. S. Koh and J. G. Yook. Exact closed-form expression of a Sommerfeld integral for the impedance plane problem. IEEE Trans. Antennas Propag., 54(9):2568–2576, 2006.

[21] J. Lai, L. Greengard, and M. O'Neil. A new hybrid integral representation for frequency domain scattering in layered media. Appl. Comput. Harmon. A., 45(2):359–378, 2018.

[22] Y. L. Li and M. J. White. Near-field computation for sound propagation above ground using complex image theory. J. Acoust. Soc. Amer., 99(2):755–760, 1996.

[23] F. Ling and J. M. Jin. Discrete complex image method for Green's functions of general multilayer media. IEEE Microw. Guided Wave Lett., 10(10):400–402, 2000.

[24] P. A. Martin. *Multiple Scattering: interaction of time-harmonic waves with N obstacles*. Number 107. Cambridge University Press, 2006.

[25] M. Ochmann. The complex equivalent source method for sound propagation over an impedance plane. J. Acoust. Soc. Amer., 116(6):3304–3311, 2004.

[26] V. I. Okhmatovski and A. C. Cangellaris. Evaluation of layered media Green's functions via rational function fitting. IEEE Microw. Wireless Comp. Lett., 14(1):22–24, 2004.

[27] F. W. J. Olver. *NIST Handbook of Mathematical Functions*. Cambridge University Press, 2010.

[28] M. O'Neil, L. Greengard, and A. Pataki. On the efficient representation of the half-space impedance Green's function for the Helmholtz equation. Wave Motion, 51(1):1–13, 2014.

[29] M. Paulus, P. Gay-Balmaz, and O. J. F. Martin. Accurate and efficient computation of the Green's tensor for stratified media. Phys. Rev. E, 62(4):5797, 2000.

[30] V. Rokhlin, Diagonal forms of translation operators for the Helmholtz equation in three dimensions. Appl. Comput. Harmon. A.. 1993 Dec 1;1(1):82-93.

[31] J. Tausch, The fast multipole method for arbitrary Green's functions, Contemp. Math., 329 (2003), pp. 307-314.

[32] B. Wang, W. Z. Zhang, W. Cai, Taylor expansion based fast multipole method for 3-D Helmholtz equations in layered media, submitted in minor revision to J. Comput. Phys., July., 2019.

[33] L. Wang, R. Krasny, and S. Tlupova, A kernel-independent treecode based on barycentric Lagrange interpolation, arXiv:1902.02250v1, Feb, 2019.

[34] G. N. Watson. *A Treatise of the Theory of Bessel Functions (second edition)*. Cambridge University Press, Cambridge, UK, 1966.

[35] E. T. Whittaker amd G. N. Watson. *A Course of Modern Analysis*. Cambridge University Press, 4th edition, 1927.

[36] T. Xia, L. L. Meng, Q. S. Liu, H. H. Gan, W. C. Chew, A low-frequency stable broadband multilevel fast multipole algorithm using plane wave multipole hybridization. IEEE Trans. Antennas Propag.. 2018 Aug 22;66(11):6137-45.

[37] L. Ying, G. Biros and D. Zorin, A kernel-independent adaptive fast multipole algorithm in two and three dimensions, J. Comput. Phys., 196 (2004), pp. 591-626.

[38] W. Z. Zhang, B. Wang, and W. Cai. Exponential convergence for multipole expansion and translation to local expansions for sources in layered media: 2-D acoustic wave. *arXiv:1809.07716*, submitted to SIAM Numer. Anal., June, 2019.

[39] W. Z. Zhang, B. Wang, and W. Cai. Fast multipole method for 3-D Laplace equation in layered media. submitted to *arXiv*, and Computer Physics Communications, August, 2019.